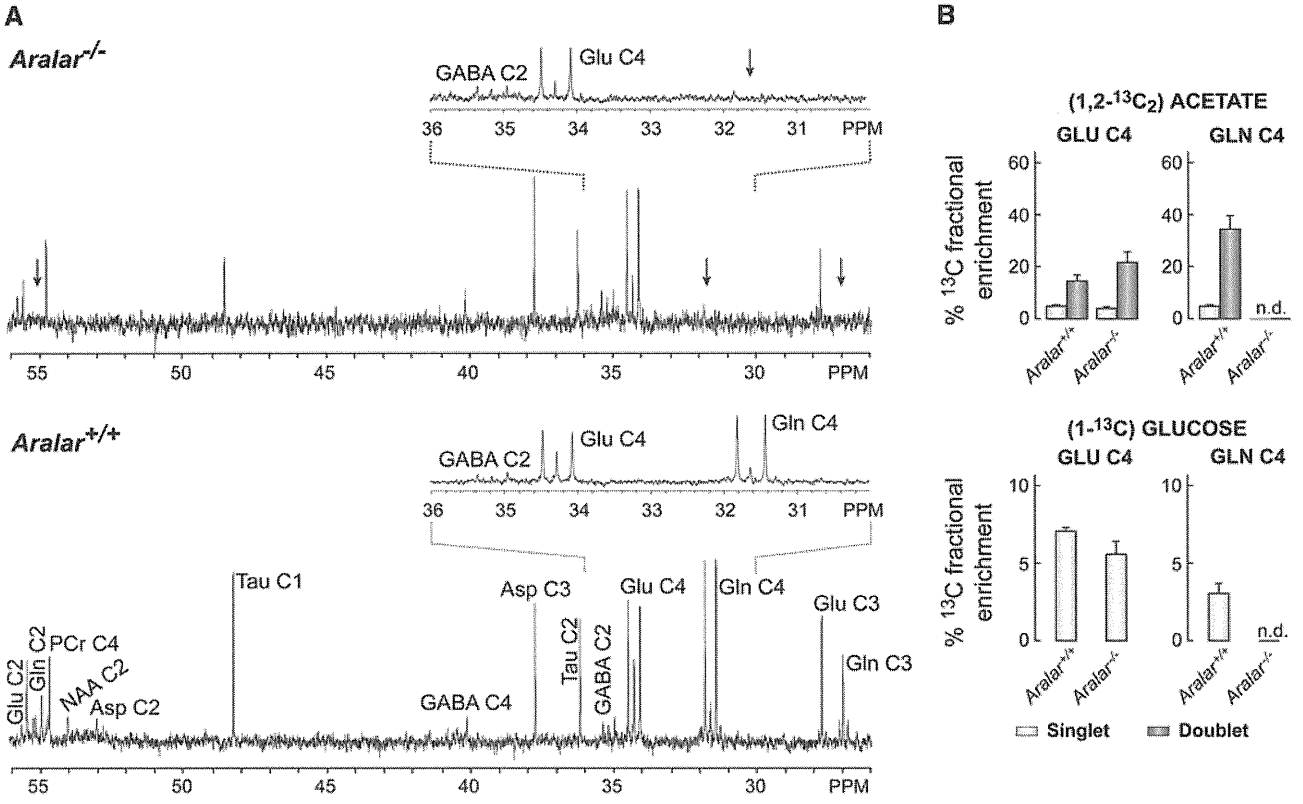

Figure 2 Lack of ^{13}C-labeled glutamine in *Aralar*$^{-/-}$ mice. (**A**) Expansions of representative proton-decoupled ^{13}C nuclear magnetic resonance spectra (125.13 MHz, 25°C, pH 7.2) of neutralized perchloric acid extracts from the cerebral tissue of control (*Aralar*$^{+/+}$) and Aralar-deficient (*Aralar*$^{-/-}$) mice intraperitoneally injected with (1,2-$^{13}C_2$) acetate. Only the 26 to 56 p.p.m. region is shown, with insets highlighting the 30 to 36 p.p.m. region. Asp, aspartate (C2: 53.0 p.p.m.; C3: 37.8 p.p.m.); GABA, γ-aminobutyric acid (C2: 35.4 p.p.m., C4: 40.4 p.p.m.); Gln, glutamine (C2: 55.0 p.p.m.; C3: 27.0 p.p.m.; C4: 31.6 p.p.m.); Glu, glutamate (C2: 55.4 p.p.m.; C3: 27.7 p.p.m.; C4: 34.2 p.p.m.); NAA, *N*-acetylaspartic acid (C2: 54.2 p.p.m.); PCr, phosphocreatine (C4′: 54.4 p.p.m.); p.p.m., parts per million; Tau, taurine (C1: 48.4 p.p.m.; C2: 36.1 p.p.m.). (**B**) Combined fractional ^{13}C enrichment of glutamate C4 and glutamine C4, of extracts from the cerebral tissue of control (*Aralar*$^{+/+}$) and *Aralar*-deficient (*Aralar*$^{-/-}$) mice injected with (1,2-$^{13}C_2$) acetate or with (1-^{13}C) glucose, determined as indicated in the text. See Cerdán *et al* (1990) for assignments of singlets and doublets. Arrows indicate the absence of Gln labeling in the KO mice extracts. Results are expressed as the mean ± s.e.m.

Astrocytes use Preferentially Aspartate as Nitrogen Donor for Glutamate and Glutamine Synthesis

There is no decrease in the levels of glutamate and glutamine in cultured astrocytes from *Aralar*-KO mice (Table 1). As the culture medium provides some essential nutrients such as glutamine, this may compensate for deficits *in vivo* and complicates the comparisons of cultured cells to *in vivo*.

The failure to synthesize glutamate and glutamine in brain astroglia could arise from a defective production of α-KG in these cells. The decrease in pyruvate levels in *Aralar*-KO neuronal cultures (final pyruvate concentrations in the culture medium drop from 19.7 ± 1.1 μmol/L in control neurons to 3.2 ± 0.6 μmol/L in *Aralar*-KO neurons) possibly also occurs *in vivo* and may result in a drain of pyruvate in astrocytes jeopardizing oxaloacetate (OAA) production by pyruvate carboxylase and subsequent α-KG formation. However, α-KG levels in cultured astrocytes from WT and *Aralar*-KO mice were the same (1.75 ± 0.4 and 1.67 ± 0.2 nmol/mg protein, respectively, $n=4$), whereas a clear increase in α-KG levels was detected in the brain from *Aralar*-KO mice (mean ± s.e.m. of four mice per group: 4.96 ± 0.16 and 13.07 ± 1.3 nmol/g weight, in WT and *Aralar*-KO mice, respectively, $P<0.001$). These results indicate that the drop in glial glutamate synthesis is not due to a lack of α-KG but most probably to a shortage of the amino-group donor.

The absence of Aralar leads to a prominent fall in brain aspartate levels (Table 3) and aspartate content of neurons in culture (Table 1) and to decreases in alanine content in brain (Table 3) and neuronal cultures (Table 1). Aspartate production requires the aspartate aminotransferase reaction, which is thought to proceed in the direction of aspartate synthesis in mitochondria and in that of OAA synthesis in the cytosol, as both enzymes are components of the malate-aspartate shuttle that drives reduction equivalents to mitochondria in an irreversible way in normally polarized mitochondria

(Berkich *et al*, 2007). The lack of Aralar removes the main pathway whereby neuronal mitochondria take up glutamate from the cytosol and this entails a fall in mitochondrial synthesis of aspartate through OAA transamination. In addition, mitochondrial aspartate cannot egress to the cytosol. On the other hand, decreases in alanine content in neurons and brain of the *Aralar*-KO mouse are likely related through alanine aminotransferase to their low pyruvate levels. We reasoned that exogenous, neuron-born aspartate or alanine may be the limiting factor for glutamate synthesis in astroglia.

To explore the role of aspartate or alanine as amino source for glutamate formation in astrocytes, we investigated glutamate and glutamine formation in primary astrocyte cultures exposed to glucose, to provide the carbon skeleton of glutamate, and different amino acids added either alone, to test for glutamate formation by astrocytes (by transamination), or in combination with glutamate, to test their role in supplying the amido nitrogen of glutamine (recycling).

The supply of 10 to 200 μmol/L aspartate to astroglial cultures resulted in glutamate (Figure 3A) and glutamine (Figure 3B) levels significantly higher than those obtained with all the other amino acids tested including alanine, BCAAs (leucine), and GABA. In fact, only aspartate, but not alanine, GABA, or leucine, was able to induce a significant increase in glutamine and glutamate synthesis. However, aspartate did not enhance glutamate or glutamine synthesis when added together with glutamate (Figures 3C and 3D). Taken together, these findings show unambiguously that aspartate is the main nitrogen source for *de novo* glutamate synthesis, but it is not used for glutamine synthesis from glutamate.

Brain glial cells have the capacity to label aspartate C3 derived from (1-^{13}C) glucose or from (1,2-$^{13}C_2$) acetate (Aureli *et al*, 1997; Preece and Cerdán, 1996). The prominent *in vivo* labeling of aspartate C3 from (1-^{13}C) glucose is due to the conversion of ^{13}C-labeled pyruvate into ^{13}C-labeled OAA and aspartate through the activity of glial pyruvate carboxylase. Surprisingly, aspartate C3 labeling from (1-^{13}C) glucose is maintained in *Aralar*-KO mice (Supplementary Figure 4). *In vivo* labeling with (1,2-^{13}C) acetate results in a prominent singlet in aspartate C3, which arises from the loss of one of the two labeled carbons in OAA formed in the first turn of the tricarboxylic acid cycle after incorporation of unlabeled acetyl-CoA moities. The prominent aspartate C3 singlet observed under these conditions is then due to unlabeled acetyl-CoA dilution occurring in the rapidly turning over glial tricarboxylic acid cycle. Remarkably, the aspartate C3 singlet formed by labeling with (1,2-^{13}C) acetate is the same in the brain from wild-type and *Aralar*-KO mice (Figure 2A). These findings clearly indicate that the glial pathway of aspartate labeling is independent of the activity of the mitochondrial aspartate–glutamate carrier and that this labeled aspartate is not used in the synthesis of their own glutamate. In contrast, labeling of aspartate C2 with (1-^{13}C) glucose, which reflects the neuronal aspartate pool (Navarro *et al*, 2008) is severely reduced in the *Aralar*-KO mouse brain (Supplementary Figure 4). Thus, even when glial cells have the capacity to label aspartate, this aspartate is unavailable for their own synthesis of glutamate, which requires an exogenous source of this amino acid. In agreement with this, the addition of aspartate results in the same stimulation of glutamate and glutamine synthesis in cultured astroglial cells from *Aralar*-WT and *Aralar*-KO mice (Figures 3E and 3F). These results provide strong support to the notion that the drastic fall in glutamine synthesis observed in the brain from *Aralar*-KO mice is not due to a constitutive failure in its synthesis by brain astrocytes but to a limitation or lack in the supply of exogenous aspartate arising from the neighboring neurons.

Discussion

The role of aspartate as glutamate and glutamine precursor in astrocytes was investigated long ago by labeling with ^{15}N (Yudkoff *et al*, 1986, 1987; Erecinska *et al*, 1993). Aspartate was rapidly taken up from the medium (Yudkoff *et al*, 1986, 1987; Erecinska *et al*, 1993), and its amino group was transferred to glutamate in the aspartate aminotransferase reaction. The newly made glutamate was the precursor of glutamine through glutamine synthetase (Yudkoff *et al*, 1987; Erecinska *et al*, 1993), a reaction taking place exclusively in the cytosol of astrocytes (Martínez-Hernandez *et al*, 1977). However, the importance of this pathway for *de novo* synthesis of glutamate in brain astroglial cells remained unknown. The results reported herein suggest that aspartate is the main nitrogen donor for glial glutamate synthesis. On the other hand, the second amino group required for glutamine synthesis, the amido group, does not directly require aspartate. This may arise from ammonia itself (released by neurons), or from glial GDH, which operates mainly in the direction of glutamate oxidation in astrocytic mitochondria, particularly in response to high external glutamate levels (McKenna, 2007; McKenna *et al*, 1996).

Although alanine levels fall in neurons (Table 1) and brain (Table 3) of the *Aralar*-KO mouse, it is unlikely that the fall in alanine causes the failure to synthesize glial glutamate. The marked preference for aspartate over alanine in glial glutamate production (Figure 3) stands against this possibility. The BCAAs do not compensate for the lack of aspartate in glial glutamate synthesis, as the fall in glutamine levels in the *Aralar*-KO mouse brain takes place in face of unchanged levels of BCAAs (Table 3) and a knockout mouse for mitochondrial-branched chain aminotransferase, the enzyme required for glial glutamate synthesis from BCAAs, has high circulating

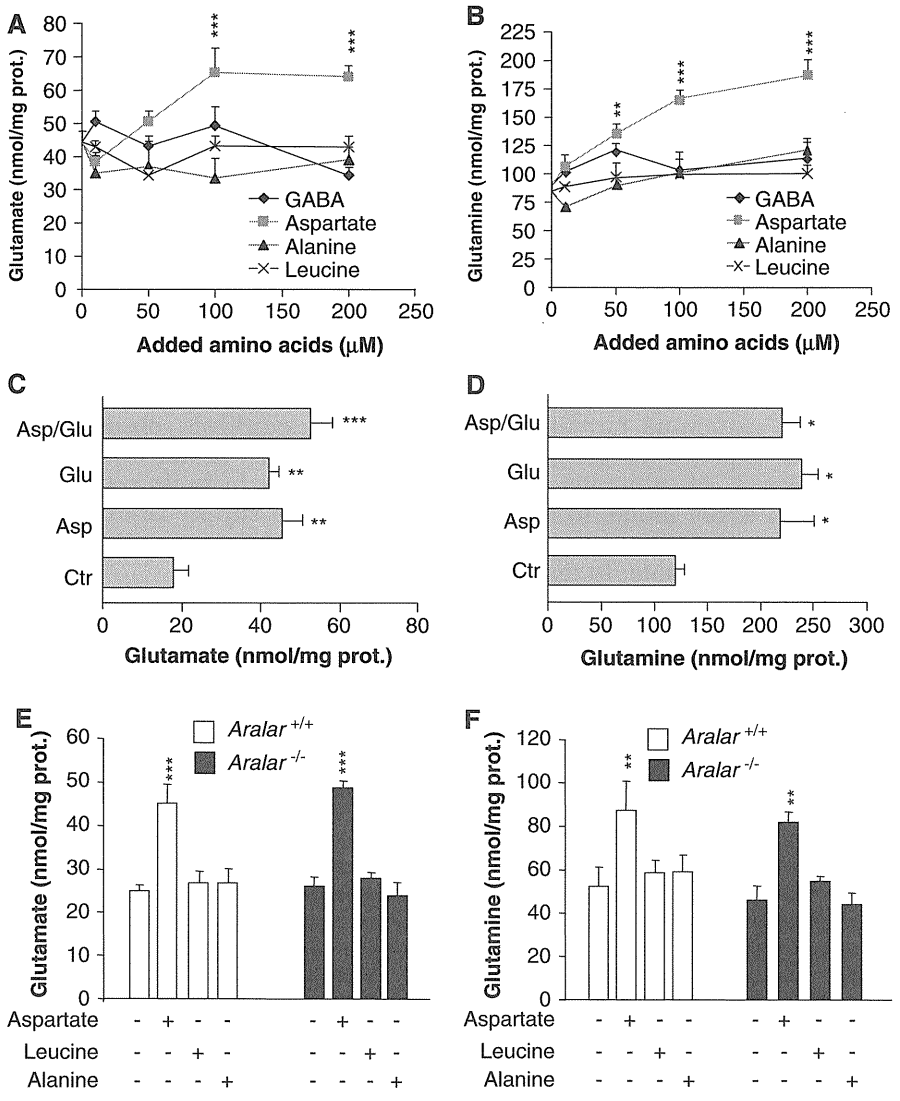

Figure 3 Aspartate promotes glutamate synthesis in astroglial cell cultures. (**A**, **B**) Cortical astrocytes cultures from wild-type (WT) mice (DIV14) were incubated for 1 hour in KRBH (140 mmol/L NaCl, 3.6 mmol/L KCl, 0.5 mmol/L NaH_2PO_4, 0.5 mmol/L $MgSO_4$, 1.5 mmol/L $CaCl_2$, 2 mmol/L $NaHCO_3$, 10 mmol/L Hepes, pH 7.4) containing 2 mmol/L glucose in the absence or presence of supplemented amino acids (γ-aminobutyric acid (GABA), aspartate, alanine, or leucine; 10 to 200 μmol/L). Cellular extracts and media were separately recovered to measure glutamate (**A**) and glutamine (**B**) content, respectively, by an enzymatic end point method. (**C**, **D**) Cortical astrocytes from WT mice (DIV14) were incubated for 1 hour in KRBH-2 mmol/L glucose (Ctr) and in the presence of added aspartate (Asp; 50 μmol/L), glutamate (Glu; 50 μmol/L) or both together (Asp/Glu). Cellular extracts and media were separately recovered to measure glutamate (**C**) and glutamine (**D**) content, respectively, as described above. Under those conditions, astroglial cultures were viable as detected by using the calcein-acetoxy methylester/propidium iodide essay. (**E**, **F**) Cortical astrocytes from WT and *Aralar*-KO mice (DIV14) were incubated for 2 hours in KRBH containing 15 mmol/L glucose in the absence or presence of 100 μmol/L aspartate, 100 μmol/L alanine, or 100 μmol/L leucine. Cellular extracts and media were separately recovered to measure glutamate (**E**) and glutamine (**F**) content, respectively, as described. Intracellular glutamate (**A**, **C**, **E**) and extracellular glutamine content (**B**, **D**, **F**) are expressed as nmol/mg protein. Results are mean ± s.e.m. ($n = 6$) of three independent experiments. Data were statistically evaluated by one-way analysis of variance followed by Student–Newman–Keuls's *t*-test method (***$P \leqslant 0.001$; **$P \leqslant 0.01$; *$P \leqslant 0.05$). KRBH, Krebs-Ringer bicarbonate-HEPES buffer.

BCAAs but has not been shown to have defects in brain glutamate or glutamine synthesis (She *et al*, 2007). Taken together, the results suggest that the fall in aspartate levels causes the decrease in astroglial glutamate and glutamine synthesis in the brain from *Aralar*-KO mice. Our results strongly support that any defect in aspartate supply may immediately have consequences on glial glutamate and glutamine synthesis. As NAA is a donor of aspartate, which is known to be transported out of neurons and its levels decrease in Aralar-deficient brain (Jalil *et al*, 2005; Wibom *et al*, 2009), we cannot exclude a role of NAA as aspartate donor for glial glutamate synthesis, although the absence of the NAA cleavage enzyme,

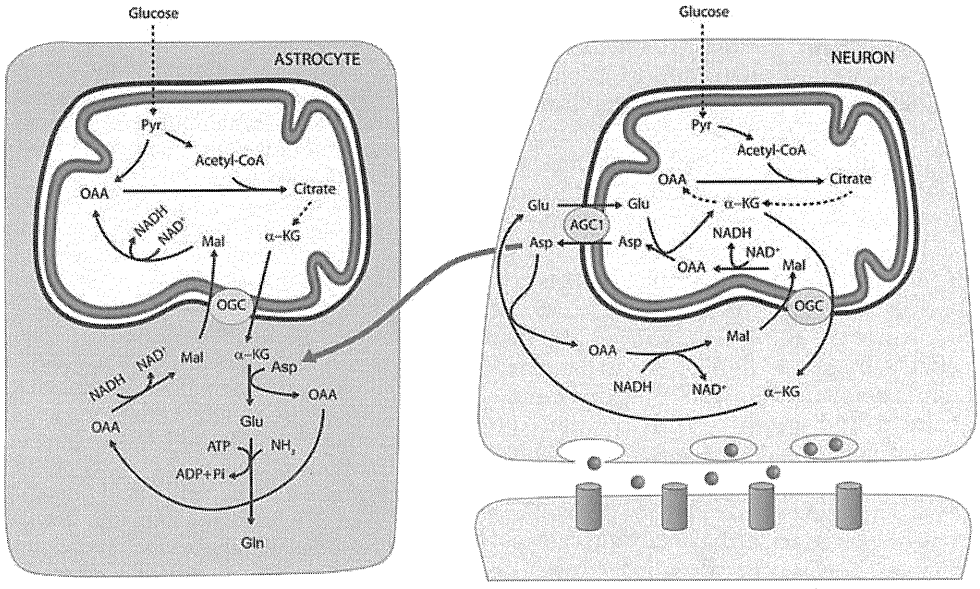

Figure 4 Neuron-to-glia transcelullar aspartate efflux pathway for glial glutamate synthesis. Neuronal mitochondria are provided with Aralar/AGC1/Slc25a12 and the oxoglutarate carrier/OGC/Slc25a11 and carry out the malate-aspartate shuttle to transfer NADH reducing equivalents to the mitochondrial matrix. AGC1 is irreversible in polarized mitochondria and the main pathway of glutamate supply to the mitochondrial matrix. As cAST functions in the direction of glutamate formation in cells with an active malate-aspartate shuttle, mitochondria are the only site where aspartate is produced (in the mitochondrial aspartate aminotransferase reaction), and aspartate leaves the matrix through AGC1 to reach the cytosol. *De novo* glutamate synthesis in astroglial cells takes place in the cytosol in the cAST reaction with aspartate as amino-nitrogen donor to α-KG. A second amino group (possibly arising from ammonia itself formed in neurons in the phosphate-activated glutaminase reaction) is acquired in the glutamine synthetase reaction and glial glutamine is now transferred to neurons along the glutamate–glutamine cycle (not shown). Oxaloacetate (OAA) arising from the cAST reaction is converted to malate, and malate entry in glial mitochondria along the OGC provides an alternative pathway for redox transfer to mitochondria, which partly compensates for the lack of a malate-aspartate shuttle in brain astrocytes. In this way, equivalent transfer to astroglial mitochondria is stoichiometrically related to *de novo* glutamate production. Alternatively, malate formed in astroglial cytosol may be transferred back to neurons, as malate is released to a higher extent from cultured astrocytes than from cultured neurons (Westergaard *et al*, 1994) (not shown). The presence of mitochondria in the fine peridentritic processes of astrocytes (Figures 1E and 1F) indicates astrocytic oxidative capability near synapses. This confirms the reports by the Nedergaard group (Lovatt *et al*, 2007) and suggests that astrocytes need not be predominately glycolytic to supply their energy during brain activation. Indeed, the labeling of Asp C3 (Supplementary Figure 4) by [1-^{13}C]glucose and its dilution by unlabeled AcCoA in the [1,2-^{13}C]acetate study indicates that astrocytes oxidize glucose and must have some redox carrier system. AGC, aspartate–glutamate carrier; Asp, aspartate; Gln, glutamine; Glu, glutamate; α-KG, α-ketoglutarate; Mal, malate; OAA, oxalacetic acid; OGC, α-ketoglutarate–malate carrier; Pyr, pyruvate.

aspartoacylase, in astrocytes (Madhavarao *et al*, 2004) makes it unlikely.

With the development of the blood–brain barrier, brain cells must rely on their own aspartate production from the first week onwards (Price *et al*, 1984). The lack of Aralar explains the progressive decline in brain aspartate that is closely followed by that of NAA, glutamine, and myelin lipids, including the major myelin lipid galactocerebroside, at a time where the central nervous system pathology of the *Aralar*-KO mouse develops (Jalil *et al*, 2005). This pathology, and that of the patient with Aralar deficiency (Wibom *et al*, 2009), is similar to the deficiency in UDP-galactose:ceramidegalactosyl transferase (Coetzee *et al*, 1996), the enzyme required for the synthesis of myelin galactocerebrosides. However, ceramidegalactosyl transferase deficiency is milder than Aralar deficiency even though there is a total lack of myelin galactocerebrosides in the ceramidegalactosyl transferase-KO mouse and only a partial loss in the Aralar-KO mouse. This suggests that the progressive failure to synthesize astroglial glutamate and glutamine is likely to contribute to the central nervous system pathology in Aralar deficiency.

Aspartate is released by neurons to the extracellular space and a vesicular transporter of aspartate is found in synaptic microvesicles (Miyaji *et al*, 2008). The preference for aspartate as nitrogen donor for glutamate synthesis may be due to: (1) the large activity of aspartate aminotransferase in astrocytes and (2) the active aspartate transport systems in the glial membrane. Brain aspartate aminotransferase has about 6 to 10 times higher activity than that of alanine or branched chain amino-acid aminotransferases (Goldlust *et al*, 1995). In addition, astrocytes have high-affinity sodium-dependent aspartate/glutamate transport systems, GLT1/EAAT2/Slc1a2, and the GLAST/EAAT1/Slc1a3 transporter (Kanner, 2006) that allows a rapid scavenging of low-micromolar

concentrations of aspartate in astrocytes (Yudkoff *et al*, 1986; Erecinska *et al*, 1993). This is not so for leucine and possibly alanine transport systems LAT2 (Bröer *et al*, 2007), which have much lower affinity (the *Km* for leucine transport in astrocytes is 400 μmol/L (Yudkoff *et al*, 1996) and being Na^+ independent, do not allow the accumulation of the transported amino acid against a concentration gradient.

Redox shuttles in astrocytes have much lower activity than those in neurons (Ramos *et al*, 2003; Berkich *et al*, 2007; Xu *et al*, 2007; Cahoy *et al*, 2008), and the relative effects of Aralar deficiency in lactate production and glucose utilization in neurons and astrocytes in culture found in this study (Table 2) strongly support a much more prominent role of the malate-aspartate shuttle in neurons than in astrocytes. This is consistent with a higher redox state of cytosolic NADH/NAD^+ in astrocytes (Kasischke *et al*, 2004), the higher standing lactate-to-pyruvate ratios in astroglial cultures (Table 2) and the ability to upregulate glycolysis because of a high 6-phosphofructo-2-kinase/fructo-2,6-bisphosphatase-3 activity in astrocytes but not in neurons (Herrero-Mendez *et al*, 2009). However, the neuron-to-astrocyte aspartate efflux pathway described herein (Figure 4) may provide a means to transfer NADH/NAD^+ redox potential to astrocyte mitochondria, as an alternative transcellular shuttle system. Indeed, aspartate uptake coupled to OAA production provides a substrate for cytosolic malate dehydrogenase resulting in NADH consumption in the cytosol and malate formation. As the α-ketoglutarate–malate carrier is equally represented in neuronal and glial mitochondria (Berkich *et al*, 2007), aspartate utilization in glutamate formation in astrocytes will be stoichiometrically related to reducing equivalent transfer to mitochondria. In this way, transcellular aspartate traffic would result in malate oxidation by astrocytic mitochondria. Whether this pathway of carbon flow from neuronal aspartate to glial OAA utilization and reducing equivalent transfer in mitochondria could contribute to the preference for aspartate in glial glutamate production remains to be established. Alternatively, malate formed in astroglial cytosol may be transferred back to neurons, as malate is released to a higher extent from cultured astrocytes than from cultured neurons (Westergaard *et al*, 1994).

Acknowledgements

The authors thank Isabel Manso and Bárbara Sesé for technical support. TBR held a fellowship from the Fundação para a Ciência e Tecnologia/Ministério da Ciência e Ensino Superior, Portugal (SFRH/BPD/26881/2006). IL-F held a fellowship from the Comunidad de Madrid, Spain.

Disclosure/conflict of interest

The authors declare no conflict of interest.

References

Aureli T, Di Cocco ME, Calvani M, Conti F (1997) The entry of [1-^{13}C]glucose into biochemical pathways reveals a complex compartimentation and metabolite trafficking between glia and neurons: a study by ^{13}C-NMR spectroscopy. *Brain Res* 765:218–27

Bak LK, Schousboe A, Waagepetersen HS (2006) The glutamate/GABA-glutamine cycle: aspects of transport, neurotransmitter homeostasis and ammonia transfer. *J Neurochem* 98:641–53

Berkich DA, Ola MS, Cole J, Sweatt AJ, Hutson SM, LaNoue KF (2007) Mitochondrial transport proteins of the brain. *J Neurosci Res* 85:3367–77

Bröer S, Bröer A, Hansen JT, Bubb WA, Balcar VJ, Nasrallah FA, Garner B, Rae C (2007) Alanine metabolism, transport, and cycling in the brain. *J Neurochem* 102:1758–70

Cahoy JD, Emery B, Kaushal A, Foo LC, Zamanian JL, Christopherson KS, Xing Y, Lubischer JL, Krieg PA, Krupenko SA, Thompson WJ, Barres BA (2008) A transcriptome database for astrocytes, neurons, and oligodendrocytes: a new resource for understanding brain development and function. *J Neurosci* 28:264–78

Cerdán S, Künnecke B, Seelig J (1990) Cerebral metabolism of [1,2-$^{13}C_2$] acetate as detected by *in vivo* and *in vitro* ^{13}C NMR. *J Biol Chem* 265:12916–26

Chapa F, García-Martín ML, García-Espinosa MA, Cerdan S (2000) Metabolism of (1-^{13}C) glucose and (2-^{13}C, 2-$^{2}H_3$) acetate in the neuronal and glial compartments of the adult rat brain as detected by [^{13}C, ^{2}H] NMR spectroscopy. *Neurochem Int* 37:217–28

Coetzee T, Fujita N, Dupree J, Shi R, Blight A, Suzuki K, Suzuki K, Popko B (1996) Myelination in the absence of galactocerebroside and sulfatide: normal structure with abnormal function and regional instability. *Cell* 86: 209–19

Contreras L, Urbieta A, Kobayashi K, Saheki T, Satrústegui J (2010) Low levels of citrin (*SLC25A13*) expression in adult mouse brain restricted to neuronal clusters. *J Neurosci Res* 88:1009–16

Cruz F, Cerdán S (1999) Quantitative ^{13}C NMR studies of metabolic compartmentation in the adult mammalian brain. *NMR Biomed* 12:451–62

Erecinska M, Pleasure D, Nelson D, Nissim I, Yudkoff M (1993) Cerebral aspartate utilization: near-equilibrium relationships in aspartate aminotransferase reaction. *J Neurochem* 60:1696–706

Gamberino WC, Berkich DA, Lynch CJ, Xu B, LaNoue KF (2007) Role of pyruvate carboxylase in facilitation of synthesis of glutamate and glutamine in cultured astrocytes. *J Neurochem* 69:2312–25

Goldlust A, Su TZ, Welty DF, Taylor CP, Oxender DL (1995) Effects of anticonvulsant drug gabapentin on the enzymes in metabolic pathways of glutamate and GABA. *Epilepsy Res* 22:1–11

Herrero-Mendez A, Almeida A, Fernández E, Maestre C, Moncada S, Bolaños JP (2009) The bioenergetic and antioxidant status of neurons is controlled by continuous degradation of a key glycolytic enzyme by APC/C-Cdh1. *Nat Cell Biol* 11:747–52

Hertz L, Kala G (2007) Energy metabolism in brain cells: effects of elevated ammonia concentrations. *Metab Brain Dis* 22:199–218

Jalil MA, Begun L, Contreras L, Pardo B, Iijima M, Li MX, Ramos M, Marmol P, Horiuchi M, Shimotsu K, Nakagawa S, Okubo A, Sameshima M, Isashiki Y, del Arco A, Kobayashi K, Satrústegui J, Saheki T (2005) Reduced

N-acetylaspartate levels in mice lacking aralar, a brain- and muscle-type mitochondrial aspartate-glutamate carrier. *J Biol Chem* 280:31333–9

Kasischke KA, Vishwasrao HD, Fisher PJ, Zipfel WR, Webb WW (2004) Neural activity triggers neuronal oxidative metabolism followed by astrocytic glycolysis. *Science* 305:99–103

Lieth E, LaNoue KF, Berkich DA, Xu B, Ratz M, Taylor C, Hutson SM (2001) Nitrogen shuttling between neurons and glial cells during glutamate synthesis. *J Neurochem* 76:1712–3

Lovatt D, Sonnewald U, Waagepetersen HS, Schousboe A, He W, Lin JH, Han X, Takano T, Wang S, Sim FJ, Goldman SA, Nedergaard M (2007) The transcriptome and metabolic gene signature of protoplasmic astrocytes in the adult murine cortex. *J Neurosci* 27:12255–66

Kanner BI (2006) Structure and function of sodium-coupled GABA and glutamate transporters. *J Membrane Biol* 213:89–100

Madhavarao CN, Moffett JR, Moore RA, Viola RE, Namboodiri MA, Jacobowitz DM (2004) Immunohistochemical localization of aspartoacylase in the rat central nervous system. *J Comp Neurol* 472:318–29

Martínez-Hernandez A, Bell KP, Norenberg MD (1977) Glutamine synthetase: glial localization in brain. *Science* 195:1356–8

McKenna MC, Tildon JT, Stevenson JH, Boatright R, Huang S (1993) Regulation of energy metabolism in synaptic terminals and cultured rat brain astrocytes: differences revealed using aminooxyacetate. *Dev Neurosci* 15:320–9

McKenna MC, Sonnewald U, Huang X, Stevenson J, Zielke HR (1996) Exogenous glutamate concentration regulates the metabolic fate of glutamate in astrocytes. *J Neurochem* 66:386–93

McKenna MC (2007) The glutamate-glutamine cycle is not stoichiometric: fates of glutamate in the brain. *J Neurosci Res* 85:3347–58

Miyaji T, Echigo N, Senoh S, Omote H, Moriyama Y (2008) Identification of a vesicular aspartate transporter. *Proc Natl Acad Sci USA* 105:11720–4

Navarro D, Zwingmann C, Butterworth RF (2008) Region selective alterations of glucose oxidation and amino acid synthesis in the thiamine-deficient rat brain: re-evaluation using $^{1}H/^{13}C$ nuclear magnetic resonance spectroscopy. *J Neurochem* 106:603–12

Palaiologos G, Hertz L, Schousboe A (1988) Evidence that aspartate aminotransferase activity and ketodicarboxylate carrier function are essential for biosynthesis of transmitter glutamate. *J Neurochem* 51:317–20

Preece NE, Cerdán S (1996) Metabolic precursors and compartimentation of cerebral GABA in vigabatrin-treated rats. *J Neurochem* 67:1718–25

Price MT, Pusateri ME, Crow SE, Buchsbaum S, Olney JW, Lowry OH (1984) Uptake of exogenous aspartate into circumventricular organs but not other regions of adult mouse brain. *J Neurochem* 42:740–4

Ramos M, del Arco A, Pardo B, Martínez-Serrano A, Martínez-Morales JR, Kobayashi K, Yasuda T, Bogónez E, Bovolenta P, Saheki T, Satrústegui J (2003) Developmental changes in the Ca^{2+}-regulated mitochondrial aspartate-glutamate carrier aralar1 in brain and prominent expression in the spinal cord. *Dev Brain Res* 143:33–46

Rodrigues TB, Granado N, Ortiz O, Cerdán S, Moratalla R (2007) Metabolic interactions between glutamatergic and dopaminergic neurotransmitter systems are mediated through D_1 dopamine receptors. *J Neurosci Res* 85:3284–93

Rothman DL, Behar KL, Hyder F, Shulman RG (2003) *In vivo* NMR studies of the glutamate neurotransmitter flux and neuroenergetics: implications for brain function. *Ann Rev Physiol* 65:401–27

Schousboe A (1981) Transport and metabolism of glutamate and GABA in neurons and glial cells. *Int Rev Neurobiol* 22:1–45

Schousboe A, Westergaard N, Sonnewald U, Petersen SB, Huang R, Peng L, Hertz L (1993) Glutamate and glutamine metabolism and compartmentation in astrocytes. *Dev Neurosci* 15:359–66

Shank RP, Bennet GS, Freytag SO, Campbell GL (1985) Pyruvate carboxylase: an astrocyte-specific enzyme implicated in the replenishment of amino acid pools. *Brain Res* 329:364–7

She P, Reid TM, Bronson SK, Vary TC, Hajnal A, Lynch CJ, Hutson SM (2007) Disruption of BCATm in mice leads to increased energy expenditure associated with the activation of a futile protein turnover cycle. *Cell Metab* 6:181–94

Sonnewald U, Westergaard N, Petersen SB, Unsgard G, Schousboe A (1993) Metabolism of [U-^{13}C] glutamate in astrocytes studied by ^{13}C NMR spectroscopy: incorporation of more label into lactate than into glutamine demonstrates the importance of the tricarboxylic acid cycle. *J Neurochem* 61:1179–82

Urenjak J, Williams SR, Gadian DG, Noble M (1993) Proton nuclear magnetic resonance spectroscopy unambiguously identifies different neural cell types. *J Neurosci* 13:981–9

Waniewski RA, Martin DL (1998) Preferential utilization of acetate by astrocytes is attributable to transport. *J Neurosci* 18:5225–33

Westergaard N, Sonnewald U, Schousboe A (1994) Release of alpha-ketoglutarate, malate and succinate from cultured astrocytes: possible role in amino acid neurotransmitter homeostasis. *Neurosci Lett* 176:105–9

Wibom R, Lasorsa FM, Töhönen V, Barbaro M, Sterky FH, Kucinski T, Naess K, Jonsson M, Pierri CL, Palieri F, Wedell A (2009) AGC1 deficiency associated with global cerebral hypomyelination. *New Engl J Med* 361:489–95

Xu Y, Ola MS, Berkich DA, Gardner TW, Barber AJ, Palmieri F, Hutson SM, LaNoue KF (2007) Energy sources for glutamate neurotransmission in the retina: absence of the aspartate/glutamate carrier produces reliance on glycolysis in glia. *J Neurochem* 101:120–31

Yudkoff M, Nissim I, Hummeler K, Medow M, Pleasure D (1986) Utilization of [^{15}N] glutamate by cultured astrocytes. *Biochem J* 234:185–92

Yudkoff M, Nissim I, Pleasure D (1987) [^{15}N]aspartate metabolism in cultured astrocytes. Studies with gas chromatography-mass spectrometry. *Biochem J* 241: 193–201

Yudkoff M, Daikhin Y, Grunstein L, Nissim I, Stern J, Pleasure D, Nissim I (1996) Astrocyte leucine metabolism: significance of branched-chain amino acid transamination. *J Neurochem* 66:378–85

Supplementary Information accompanies the paper on the Journal of Cerebral Blood Flow & Metabolism website (http://www.nature.com/jcbfm)

Journal of Neuroscience Research

Journal of Neuroscience Research 89:2008–2017 (2011)

Deficiency of the Mitochondrial Transporter of Aspartate/Glutamate Aralar/AGC1 Causes Hypomyelination and Neuronal Defects Unrelated to Myelin Deficits in Mouse Brain

Milagros Ramos,[1,2] Beatriz Pardo,[1] Irene Llorente-Folch,[1] Takeyori Saheki,[3] Araceli del Arco,[1,4] and Jorgina Satrústegui[1]*

[1]Departament of Molecular Biology, Centre for Molecular Biology Severo Ochoa UAM-CSIC, and CIBER of Rare Diseases (CIBERER), Autonomous University of Madrid, Madrid, Spain
[2]Centre for Biomedical Technology (Polytechnical University of Madrid), Madrid, Spain
[3]Institute for Health Sciences, Tokushima Bunri University, Tokushima, Japan
[4]Area of Biochemistry, Regional Centre for Biomedical Research (CRIB), Faculty of Environmental Sciences and Biochemistry, University of Castilla-La Mancha, Toledo, Spain

The aralar/AGC1 knockout (KO) mouse shows a drastic decrease in brain aspartate and N-acetylaspartate levels and global hypomyelination, which are attributed to the lack of neuron-produced NAA used by oligodendrocytes as precursor of myelin lipid synthesis. In addition, these mice have a gradual drop in brain glutamine synthesis. We show here that hypomyelination is more pronounced in gray than in white matter regions. We find a lack of neurofilament-labelled processes in hypomyelinated fiber tracks from cerebral cortex but not from those of the cerebellar granule cell layer, which correspond to Purkinje neurons. Therefore, the impaired development or degeneration of neuronal processes in cerebral cortex is independent of hypomyelination. An increase in O4-labelled, immature oligodendrocytes is observed in gray and white matter regions of the aralar KO brain, suggesting a block in maturation compatible with the lack of NAA supplied by neurons. However, no defects in oligodendrocyte maturation were observed in in-vitro-cultured mixed astroglial cultures. We conclude that the primary defect of pyramidal neurons in cerebral cortex is possibly associated with a progressive failure in glutamatergic neurotransmission and may be among the main causes of the pathology of aralar/AGC1 deficiency.

Key words: aralar/AGC1; aspartate-glutamate mitochondrial carrier; N-acetyl aspartate; glutamine; oligodendrocyte; neurofilaments; myelination; OmniBank

Mitochondrial metabolite carriers have a known role in the exchange of nucleotides, coenzymes, and metabolites across the mitochondrial membrane. Mutations or disruptions in the genes coding for these transporters are expected to affect this intracellular traffic, and the outcome at the cellular level can be predicted from basic biochemical and cell biology principles. However, in the case of AGC1/aralar, disruption of the gene in mouse and lack-of-function mutations in humans have revealed unanticipated new functions of the carrier. These functions are related to a complex metabolite traffic among cells with different levels of expression of the carrier whereby metabolites produced in the AGC1-enriched cells are required in the AGC1-deficient cells.

Aralar/AGC1/Slc25a12 (also named *aralar1*) and citrin/AGC2/Slc25a13 are isoforms of the mitochondrial aspartate-glutamate carrier, which 1) is a component of the malate-aspartate NADH shuttle (MAS), in which it transfers aspartate out of mitochondria in exchange of the entry of glutamate, the only irreversible step of MAS in polarized mitochondria; 2) is a mitochondrial transporter involved in the respiration on malate plus glutamate; and 3) is a component of the urea cycle in liver (LaNoue and Tischler, 1974). Disruption of aralar/AGC1, the main AGC isoform in brain and skeletal

Contract grant sponsor: Ministerio de Educacion y Ciencia; Contract grant number: BFU2008-04084/BMC (to J.S.); Contract grant sponsor: Comunidad de Madrid; Contract grant number: S-GEN-0269-2006 MITOLAB-CM (to J.S.); Contract grant sponsor: Fundacion Medica Mutua Madrileña (to B.P.); Contract grant sponsor: Fundación Ramón Areces (to CSIC-UAM).

*Correspondence to: Jorgina Satrústegui, Departamento de Biología Molecular, Centro de Biología Molecular "Severo Ochoa" UAM-CSIC, c/ Nicolás Cabrera 1, Universidad Autónoma de Madrid, Cantoblanco, Madrid 28049, Spain. E-mail: jsatrustegui@cbm.uam.es

Received 15 December 2010; Revised 31 January 2011; Accepted 8 February 2011

Published online 23 May 2011 in Wiley Online Library (wileyonlinelibrary.com). DOI: 10.1002/jnr.22639

muscle, was predicted to block MAS activity and respiration on glutamate and malate in mitochondria from these tissues if no compensatory increases in citrin/AGC2 levels existed. Indeed, in aralar/AGC1 KO mice, MAS activity was completely absent in mitochondria from these tissues (Jalil et al., 2005). Moreover, a very drastic decrease in respiration on malate plus glutamate was similarly found, although a residual activity of about 12% persisted (Jalil et al., 2005), probably explained by the presence of other glutamate carriers (GC1 or GC2) that have a much lower activity level than Aralar in these mitochondria (Molinari et al., 2005, 2009). This result is important in showing the very large contribution of AGC1 as a mitochondrial transporter of glutamate in these tissues. However, other characteristics of the aralar/AGC1 KO mouse were entirely unanticipated. These characteristics affect myelin formation and glutamine synthesis (Satrústegui et al., 2007a,b; Pardo et al., 2011).

Aralar KO mice are smaller than their littermates aralar (+/+) or aralar (+/–) and have a shortened life span of about 22–23 days. They have clear motor coordination defects, which become apparent at about 15 days, when their littermates acquire the ability to perform these tasks (Jalil et al., 2005). The brain is hypomyelinated, and this particular defect has been associated with a fall in N-acetylaspartate (NAA) levels in whole brain and cultured neurons from aralar (–/–) mice (Jalil et al., 2005). Based on the fact that NAA can be used as an acetate donor for myelin lipid synthesis (Mehta and Namboodiri, 1995; Chakraborty et al., 2001), it was proposed that the failure of aralar-deficient neurons to provide this lipid precursor to oligodendrocytes could result in a limited synthesis of galactocerebrosides, a major component of myelin lipids, and in hypomyelination (Jalil et al., 2005; Satrústegui et al., 2007b). The mouse deficient in UDP-galactose:ceramide galactosyltransferase (CGT), the enzyme responsible for the synthesis of galactocerebrosides (Coetzee et al., 1996; Bosio et al., 1996), has a shortened life span and progressive defects in myelin properties (Coetzee et al., 1998; Marcus et al., 2000), all of which are rescued by oligodendrocyte-specific expression of CGT (Zöller et al., 2005). However, the phenotype of the aralar KO mouse is much more severe than that of the CGT-KO mouse, indicating that aralar deficiency causes additional defects. Indeed, we have found that, because of the drop in neuronal aspartate levels, a gradual failure of glutamate-glutamine cycle develops in these animals, which is likely to contribute to the severity of the phenotype (Pardo et al., 2011). A human AGC1-deficient patient has been described with a pathology resembling that of the aralar KO mouse, including global cerebral hypomyelination and a drop in brain NAA (Wibom et al., 2009). This indicates that NAA may have a similar role in myelin lipid synthesis in mouse and humans.

We have analyzed here in more detail brain hypomyelination and axonal processes in aralar KO mice and studied the growth and maturation in culture of oligodendrocytes from these mice. The data obtained show that aralar deficiency has a clear impact on the generation/degeneration of axonal processes in cerebral cortex, but not in Purkinje neurons, and that these axonal defects are primary ones, not caused by hypomyelination. The results are discussed in the light of a recent description of a new aralar KO mouse (Sakurai et al., 2010) and new findings regarding synthesis and breakdown of NAA in brain and its role in the synthesis of myelin lipids, in particular the identification of aspartate N-acetyltransferase, the enzyme responsible for NAA synthesis in brain, as NaTL8, a methamphetamine-induced neuronal protein (Niwa et al., 2007; Wiame et al., 2010; Ariyannur et al., 2010a).

MATERIALS AND METHODS

Animals and Genotypes

Male SVJ129 × C57BL6 mice carrying a deficiency for aralar expression [*Aralar* (–/–), *Aralar* (+/–), and *Aralar* (+/+)] obtained from Lexicon Pharmaceuticals were used (Jalil et al., 2005). The mice were housed in a humidity- and temperature-controlled room on a 12-hr light/dark cycle, receiving water and food ad libitum. Genotype was determined by PCR using genomic DNA obtained from tail or embryonic tissue samples (Nucleospin Tissue Kit; Macherey-Nagel) as described previously (Jalil et al., 2005). The experimental protocols used in this study were approved by the appropriate institutional review committees and met the guidelines of the proper government agency. All efforts were made to minimize animal suffering.

Brain Sections

Twenty-day-old aralar (+/+) or aralar (–/–) mice (Jalil et al., 2005) were anesthetized with an overdose of chloral hydrate and intracardially perfused with freshly prepared, buffered 4% paraformaldehyde (in 0.1 M phosphate buffer, pH 7.4). Brains were removed, postfixed for 24 her in the same fixative at 4°C, and then equilibrated in 0.1 M phosphate buffer containing 30% sucrose for 24–48 hr at 4°C. Serial 30-μm-thick coronal sections were collected with a freezing microtome and stored in cryoprotectant solution until immunohistochemistry.

For immunohistochemistry, endogenous peroxidase was first quenched in 3% H_2O_2 in 10% methanol in phosphate-buffered saline (PBS) for 20 min, and free-floating sections were blocked for 1 hr in PBS containing 10% normal horse serum, 0.25% Triton X-100 and incubated overnight at 4°C with antibodies against neurofilament 200 kDa (NF-200; 1:500; Chemicon, Temecula, CA), myelin associated glycoprotein (MAG; 1:500; Santa Cruz Biotechnology, Santa Cruz, CA), myelin/oligodendrocyte specific protein (MOSP; 1:1,000; Chemicon), neuronal nuclei (NeuN; 1:500; Chemicon), synaptophysin (1:100; Chemicon), calbindin (1:200; Sigma, St. Louis, MO), and oligodendrocyte marker O4 (O4; 1:100; Chemicon). Afterward, sections were rinsed three times in PBS and then incubated for 2 hr with the secondary biotinylated antibodies (horse anti-mouse and goat anti-rabbit; 1:150; Vector, Burlingame, CA) for 1 hr, followed by a 1-hr

reaction with avidin-biotin peroxidase complexes (regular Vectastain ABC Kit; Vector). Sections were then developed using 0.05% 3,3-diaminobenzidine (Sigma) as a chromogen in the presence of 0.03% H_2O_2 in PBS for 2–10 min. Sections were mounted onto polylysine-coated slides, dehydrated, delipidated, and coverslipped with DPX

For immunohistofluorescence: free-floating sections were blocked for 1 hr in PBS containing 10% normal horse serum, 0.25% Triton X-100 and incubated overnight at 4°C with the Cy3-conjugated antibody against glial fibrillary acidic protein (GFAP; 1:400; Sigma). Sections were rinsed three times in PBS and mounted onto polylysine-coated slides. The slides were dried overnight and coverslipped with Mowiol.

Glial Cell Cultures

Mixed macroglial (astrocytes and oligodendrocytes) cultures were obtained from 1–2-day old mice as described by McCarthy and De Vellis (1980). Briefly, cerebral cortex were dissected and mechanically dissociated in HBSS medium without Ca^{2+} and Mg^{2+} (5.33 mM KCl, 0.44 mM KH_2PO_4, 138 mM NaCl, 0.3 mM Na_2HPO_4, glucose 5.6 mM). Dissociated cells were collected by centrifugation (800*g*, 5 min) and plated in DMEM supplemented with 10% fetal bovine serum, 2 mM glutamine, and antibiotics at a density of 100,000 cells/cm^2 (low-density cell cultures) or 200,000 cells/cm^2 (high-density cell cultures) in plates precoated with poly-L-lysine. The cultures were maintained at 37°C and 95% humidity in a 7% CO_2 atmosphere for periods of 7, 14, and 21 days. The medium was changed after the first 3 days and three times per week thereafter.

Immunocytochemistry

Cells were fixed in freshly prepared 4% paraformaldehyde (in 0.1 M phosphate buffer, pH 7.4). Fixed cells were blocked for 1 hr in PBS containing 10% normal horse serum, 0.25% Triton X-100, and incubated overnight at 4°C with monoclonal antibodies against myelin basic protein (MBP; 1:50; Serotec, Bicester, United Kingdom) and galactocerebroside C (GalC; 1:500; Sigma). For DAB detection, cells were rinsed and incubated with biotinylated horse anti-mouse antibody (1:100; Vector) for 1 hr at room temperature and developed after incubation with standard ABC reagent (Vector) and nickel-intensified DAB reaction. Cell nuclei were counterstained with Hoechst 33258 (Molecular Probes, Eugene, OR) at 0.2 mg/ml in PBS. Oligodendrocytes present in high-density cell cultures were stained for MBP and GalC to analyze their maturation state. Low-density cultures were used to determine the percentage of oligodendrocytes (GalC) over total cells (Hoechst).

RESULTS

Myelin Defects Are More Prominent in Gray Than in White Matter Regions

As observed previously, myelin markers were notably reduced in the brain of the 19–21-day-old aralar KO mouse, whereas no detectable changes in neuronal numbers were observed by cresyl violet staining (Jalil et al., 2005) or NeuN immunolabeling (results not shown). In

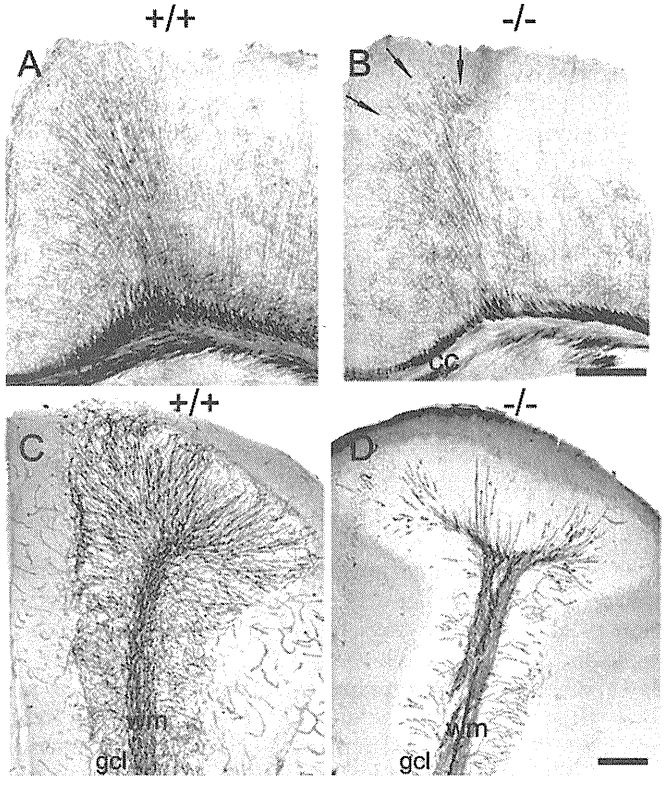

Fig. 1. Hypomyelination in gray matter regions of aralar (–/–) mice. Coronal sections stained for MAG showing the frontal cortex (**A,B**) and cerebellum (**C,D**) from 20-day-old wild-type (+/+; A,C) and aralar KO (–/–; B,D) mice. Sections from aralar KO stained for MAG show a clear hypomyelination in corpus callosum (cc), external layers of cerebral cortex (arrows in B), and cerebellar granule cell layer (gcl). Scale bars = 200 μm in B (applies to A,B); 75 μm in D (applies to C,D).

wild-type animals, myelinated fibers stained with anti-MAG (Fig. 1A) or anti-MBP antibodies (not shown) from the subcortical white matter (corpus callosum) extend up to the more external layers of the cerebral cortex, but not in aralar KO mice (Fig. 1B). Similarly, in KO animals, these fibers do not extend across the granular cell layer in the cerebellum (compare wild-type and KO in Fig. 1C,D). However, myelin labelling is lower but is still observed in the subcortical white matter (Fig. 1B) and white matter regions in the cerebellum (Fig. 1C,D), indicating that aralar deficiency does not affect gray and white matter regions equally. In addition, there are differences in myelin labelling between different white matter regions (compare white matter myelin labelling in aralar KO mouse in Fig. 1B,D).

Myelin Defects Are Independent of Axonal Changes

To study possible axonal changes associated with myelin loss, neurofilament distribution in hypomyelinated regions was studied with an anti-NF200 antibody, which recognizes mainly axonal structures (Butt et al.,

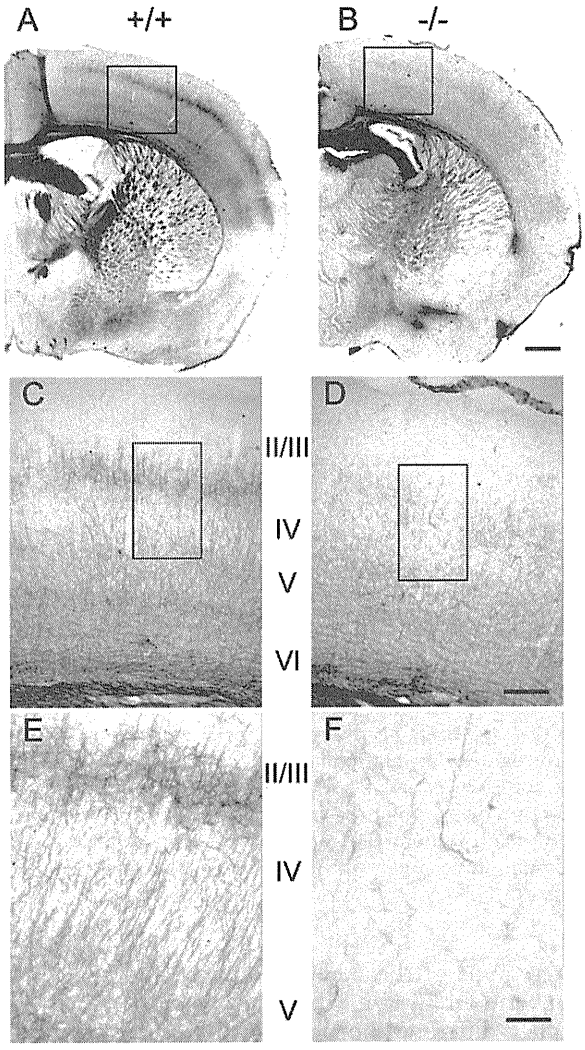

Fig. 2. Neurofilament staining in cerebral cortex of aralar (–/–) mice. Coronal brain sections of 20-day-old wild-type (+/+; **A,C,E**) and aralar KO (–/–; **B,D,F**) mice were stained with NF-200 antibody, which mainly recognizes axonal structures. Boxed areas of cortex in A and B are shown at higher magnification in C and D, respectively. Boxed areas in C and D are shown at higher magnification in E and F, respectively. High-power photomicrographs of NF200 immunoreactivity show processes from large pyramidal neurons in the lower part of cortical layer III in wild-type brain (A,C,E), which are visibly less stained in aralar KO mouse (B,D,F). Scale bars = 0.5 mm in B (applies to A,B); 100 μm in D (applies to C,D); 50 μm in F (applies to E,F).

1997). Figure 2 shows a prominent loss of neurofilaments in cerebral cortex layers IV and III in the brain of 20-day-old aralar KO mice. A reduced number of neurofilaments in the external cortex layers was also reported by Sakurai et al. (2010) in 13- or 14-day-old aralar KO mice and was taken as an indication of either a defect in the development of some nerve processes or neurodegeneration in the aralar KO mouse. Similarly, in the striatum gray matter of the aralar KO mouse, there

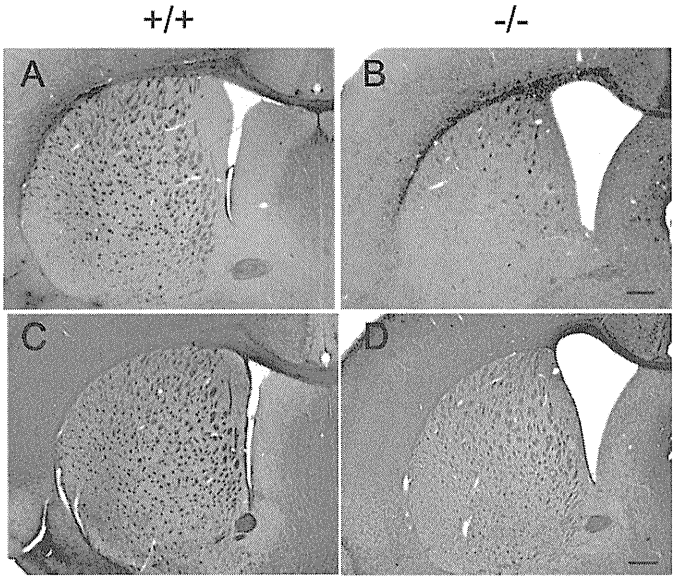

Fig. 3. Myelin and neurofilaments in striatum of aralar (–/–) mice. Coronal brain sections of 20-day-old wild-type (+/+; **A,C**) and aralar KO (–/–; **B,D**) mice were stained for myelin with an anti-MOSP antibody (A,B) and for neurofilaments with NF-200 antibody (C,D). Scale bars = 0.25 mm. [Color figure can be viewed in the online issue, which is available at wileyonlinelibrary.com.]

is a loss of myelinated fiber tracts accompanied by a partial reduction of neurofilaments staining (Fig. 3).

However, no loss of neurofilaments was observed in the cerebellum of the aralar KO mouse (Fig. 4). On the contrary, there was an increased density of NF200 fibers across the granular cell layer and in white matter regions (Fig. 4B). Strikingly, a prominent loss of NF200 fibers surrounding the Purkinje cell bodies was observed in the KO mouse (Fig. 4D). This was not due to a loss in Purkinje neurons, insofar as no loss was observed when these cells were labelled with anticalbindin antibodies (Fig. 4E–H). Therefore, the increase in the density of NF200 fibers in the granule cell layer is probably associated with increase in calbindin-labelled processes in this same region (Fig. 4F,H), and the reduced number of NF200 fibers around Purkinje cell bodies (Fig. 4D) may reflect a relative decrease in afferent basket cell fibers, although no obvious change in synaptophysin-labelled terminals on Purkinje neurons was observed (results not shown).

Because hypomyelination in the cerebellum is not associated with an equivalent loss of neurofilaments, it may be concluded that the loss of neurofilaments in cerebral cortex and striatum gray matter is not caused by hypomyelination but is due to an effect of AGC1 deficiency per se in cortical and striatal neuronal processes.

Maturation of Oligodendrocytes in Brain From Aralar-Deficient Mice

To study whether the lack of myelin was associated with changes in the distribution and morphology of oligodendrocytes, brain sections were immunolabeld with

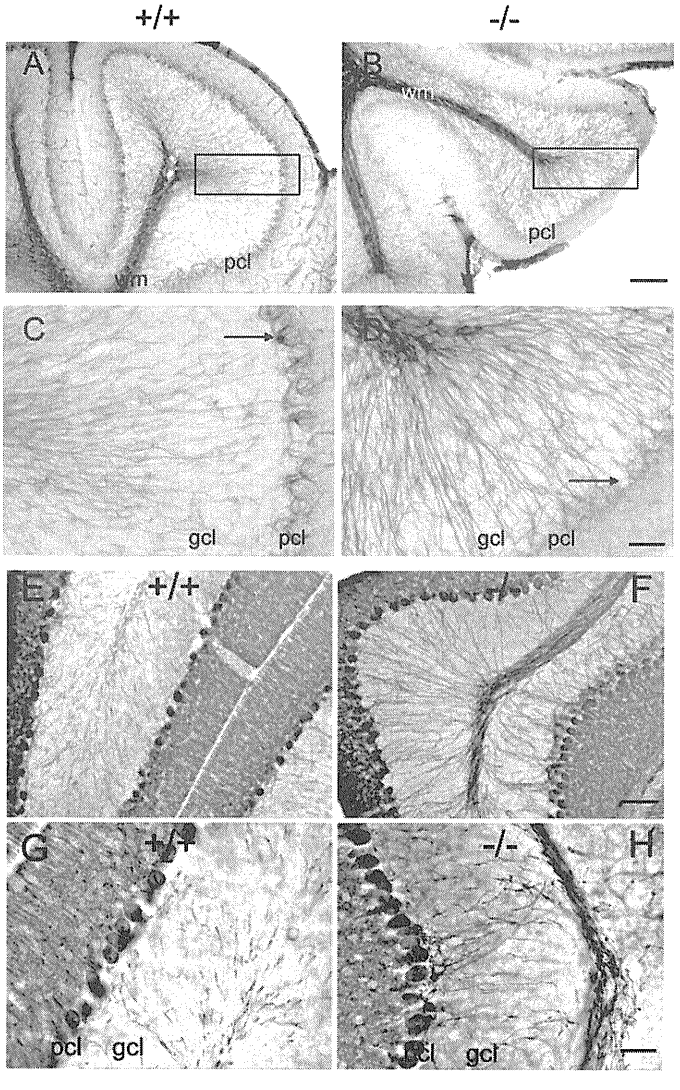

Fig. 4. Neurofilaments and calbindin-labelled Purkinje neurons in cerebellum of aralar (−/−) mice. Coronal sections of the cerebellum of 20-day-old wild-type (+/+; **A,C,E,G**) and aralar KO (−/−; **B,D,F,H**) mice. Sections were stained for neurofilaments with NF-200 antibody (A–D) and for calbindin (E–H), showing the presence of Purkinje cells in both wild-type (E,G) and aralar KO (F,H) mice. Boxed areas in A and B are shown at higher magnification in C and D, respectively. Areas similar to those shown in E and F are shown at higher magnification in G and H, respectively. Note the decrease in staining intensity of basket cell axons that surround Purkinje cells in aralar KO mouse (arrow in D) compared with wild-type mouse (arrow in C). gcl, Granular cell layer; pcl, Purkinje cell layer; wm, white matter region. Scale bars = 100 μm in B (applies to A,B); 25 μm in D (applies to C,D); 50 μm in F (applies to E,F); 25 μm in H (applies to G,H).

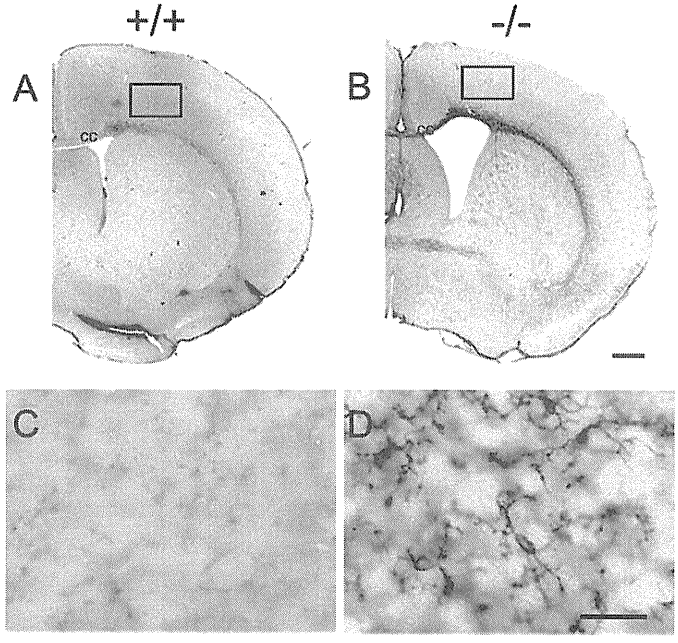

Fig. 5. Immature oligodendrocytes in brain from aralar (−/−) mice. Coronal brain sections of 20-day-old wild-type (+/+; **A,C**) and aralar KO (−/−; **B,D**) mice were stained with an anti-O4 antibody, which recognizes mainly premyelinating oligodendrocytes. Boxed areas of cortex in A and B are shown at higher magnification in C and D, respectively. Note the increased immunoreactivity for O4 in aralar KO brain sections (D) compared with wild-type (C). cc, Corpus callosum. Scale bars = 0,5 mm in B (applies to A,B); 20 μm in D (applies to C,D).

antibodies against O4, a sulfatide and pro-oligodendroblast antigen that has been used as marker of cell bodies and processes of late precursors and immature premyelinating oligodendrocytes (Sommer and Schachner, 1981; Dawson et al., 2000; Woodruff et al., 2001). O4-marked cells are clearly present in the mutant mice within gray matter regions of the cerebral cortex (Fig. 5A–D), cerebellum, and brainstem (data not shown), albeit with a somewhat different morphology and increased intensity of staining, which may suggest a difference in maturation with respect to the control mice. A similar labeling pattern was obtained by using myelin oligodendrocyte-specific protein (MOSP) as oligodendrocyte cell marker (Dyer et al., 2000; results not shown). Moreover, staining of white matter tracts with O4 antibodies was also stronger in KO mice (see the corpus callosum in Fig. 5A,B). This may suggest that oligodendrocytes are formed in the right numbers but that their differentiation is stalled in the KO mouse.

Interestingly, there is a similar increase in oligodendrocyte numbers in the CGT knockout mouse, which lacks myelin galactolipids (Marcus et al., 2000). CGT-deficient oligodendrocytes express immature forms of myelin-associated glycoprotein (MAG) even in the older animals, a clear indication of an impeded maturation (Marcus and Popko, 2002).

Astrogliosis in Aralar KO Mouse

Aralar (−/−) brain sections exhibited elevated staining for glial acidic fibrillary protein (GFAP) compared with wild-type mice (Fig. 6A–H). Astrogliosis was particularly prominent in subcortical white matter (Fig. 6A–H), in

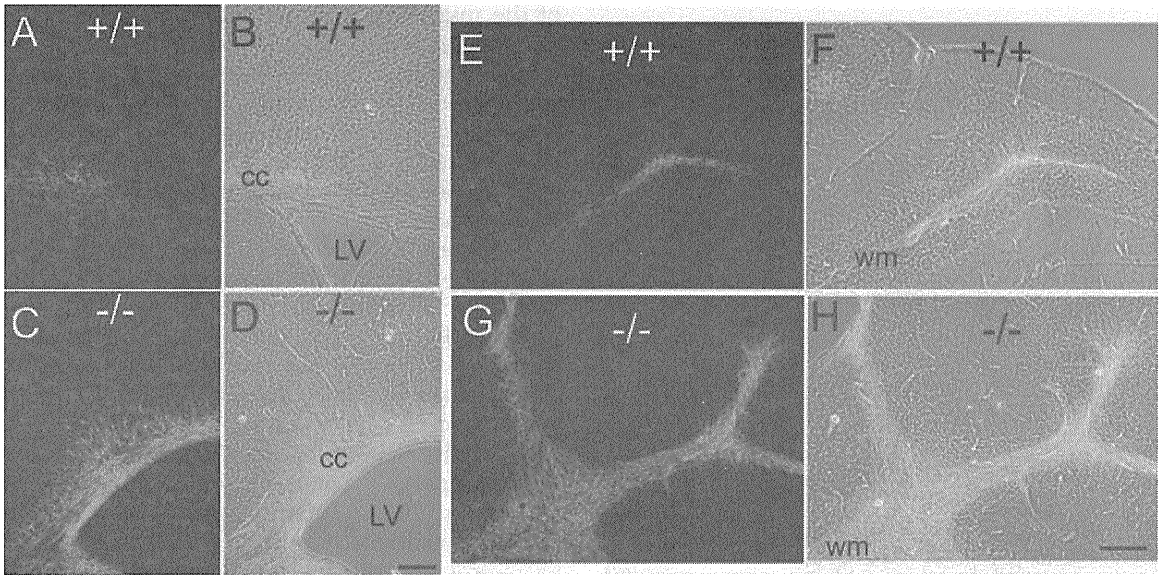

Fig. 6. Astroglyosis in aralar (–/–) mice. Coronal brain sections showing the frontal cortex (**A–D**) and cerebellum (**E–H**) from 20-day-old wild-type (A,B,E,F) and aralar KO (C,D,G,H) mice. Sections were stained with a GFAP-Cy3 antibody (A,C,E,G). Transmission light microphotographs of A,C,E,G are shown merged with fluorescent images in B,D,F,H, respectively, to reveal the morphology of the sections. Note the enlarged ventricles (LV) and the increased staining for GFAP in aralar KO mice, both in the subcortical white matter (C) and in the cerebellum white matter (G). cc, Corpus callosum; LV, lateral ventricles; wm, white matter region. Scale bars = 100 μm in D (applies to A–D); 100 μm in H (applies to E–H).

cerebellar white matter (Fig. 6E–H), and within the white matter of the spinal cord (not shown). Astrogliosis was especially acute in those animals with advanced CNS pathology (ventricle enlargement, severe reduction in the number of myelinated axons) but was less or hardly apparent in those with a milder pathology. Astrogliosis in white matter regions was also reported in the CGT-KO mouse, but also as a late effect, when a substantial loss of myelin proteins is observed (Coetzee et al., 1998). In the aspartoacylase KO mouse (Mattan et al., 2010), a model of Canavan disease, which lacks of the enzyme reponsible for NAA cleavage in the oligodendrocyte, there is a similar increase in brain GFAP levels and hypertrophic astrocytes starting at about the time when the decrease in myelination becomes apparent (Mattan et al., 2010). In sum, the increased GFAP immunostaining in the aralar KO mouse is restricted to white matter regions and is probably secondary to hypomyelination. However, further studies will be required to determine whether astrogliosis in the aralar KO mouse is reactive or causative.

Oligodendrocyte Maturation in Culture

Oligodendrocytes have very low levels of aralar mRNA compared with neurons (Cahoy et al., 2008), so it was postulated that the inability of aralar-deficient oligodendrocytes to mature and myelinate in vivo, especially in gray matter regions, was due to the lack of supply of NAA from neighboring neurons. To test whether the lack of aralar caused a primary failure in oligodendrocyte maturation in a neuron-free medium, mixed glial cultures were obtained from KO animals and studied during maturation in culture at different cell densities. Serum was present in the culture medium.

The percentage of oligodendrocytes within the total glial population was about 20% between 7 and 21 days in vitro, as judged from the immunolabeling with anti GalC antibodies. This percentage was the same in control and mutant mice (Fig. 7A). The maturation state of the oligodendrocytes was studied in higher density cultures (200,000 cells/cm^2) and was evaluated at 21 days in vitro, after labeling with anti-GalC and anti MBP antibodies. Figure 7 clearly shows that there was no difference in the maturation state between mutant (Fig. 7C,E) and control (Fig. 7B,D). Therefore, when cultured in a serum-rich medium, which contains fatty acids and other lipids, maturation of oligodendrocytes from aralar KO was unimpaired.

DISCUSSION

Two aralar KO mice have been generated so far, and they differ in the disruption sites and mouse strains used, intron 13 and hybrid sv129 × C57BL/6 by Jalil et al. (2005) and exon 1 and pure C57BL/6 by Sakurai et al. (2010). However, both have a similar phenotype, indicating that the effects of the disruption are not compensated by the influence of modifying genes polymorphic between the two strains. Most of the aralar (–/–) mice die at about postnatal day 22–23 regardless of the genetic background, although we have observed that a few of these animals in the hybrid sv129 × C57BL/6 occasionally reach 27–30 days. The similar penetrance of

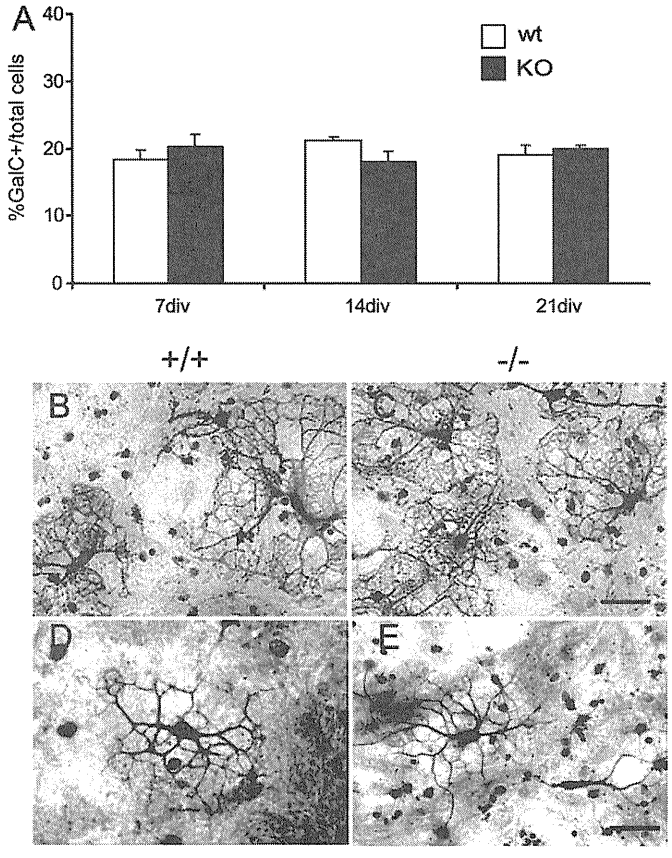

Fig. 7. Maturation of oligodendrocytes in mixed glial cell cultures. **A:** Percentage of oligodendrocytes (GalC-positive cells) present in mixed glial cell cultures obtained from postnatal 2-day-old wild-type (WT) and aralar KO (KO) mice. Cells were plated at 100,000 cells/cm^2 for 7, 14, and 21 days in vitro. Percentage of oligodendrocytes was determined by immunocytochemistry in double-stained GalC and Hoechst cultures. Data were obtained from triplicate experiments and are expressed as mean ± SEM (*$P < 0.05$, ANOVA, Tukey test). **B–E:** Mixed glial cell cultures obtained from postnatal 2-day-old wild-type (+/+; B,D) and aralar KO mice (–/–; C,E) were plated at 200,000 cells/cm^2 for 21 days in vitro. Microphotographs show oligodendrocytes stained for MBP (B,C) and GalC (D,E). No differences in the maturation state between wild-type (B,D) and aralar KO (C,E) genotypes were observed. Scale bar = 50 μm; in C (applies to B,C); 50 μm; in E (applies to D,E).

this disruption in different genetic backgrounds makes the aralar KO mice powerful models for the study of human AGC1 deficiency (Wiborn et al., 2009).

At 20 days, these animals have a pronounced loss of neurofilament-containing processes in striatum and especially cerebral cortex, in layers II/III and IV, a loss that Sakurai et al. (2010) found already at an earlier stage, 13–14 days. Interestingly, neurofilament loss is not general for all neurons in the aralar KO brain, insofar as no loss of neurofilaments in cerebellar Purkinje neurons was observed at postnatal day 20. A pronounced loss of myelinated fibers was observed in all of these gray matter regions in the aralar KO mouse, so these results clearly show that the loss of neuronal processes is independent of the myelination defect and possibly reflects a defect in the development or neurodegeneration of cerebral cortex and striatal neurons caused by the lack of aralar expression. On the other hand, Sakurai et al. (2010) reported an altered cell alignment in the Purkinje cell layer of aralar KO mice at 13–14 days, which was not observed in this study, possibly because of the older age of the mice.

When studied in culture, cortical neurons from aralar (–/–) mice have profound metabolic disturbances, including a failure to produce aspartate, which limits NAA production and may even limit protein synthesis, and a complete shutdown of the malate-aspartate NADH shuttle, which causes an increase in lactate production and a decrease in pyruvate levels (Pardo et al., 2011). Many cortical neurons are glutamatergic and rely on an active glutamate-glutamine cycle with neighboring astrocytes to maintain glutamatergic transmission. In fact, glutamate is produced de novo in astrocytes and transferred to neurons in the form of glutamine, where it is transformed to glutamate. Glutamate released from neuronal synapses can be transported into astrocytes to be transformed into glutamine, thus closing the cycle. Any glutamate leaving this cycle must be replaced by de novo synthesis in astrocytes. When glutamate is metabolized in neurons, it leaves the cycle, and an amino group must be transferred into astrocytes for de novo synthesis of glutamate. We have shown that aspartate (or NAA) produced by neurons is required in neighboring astrocytes as a nitrogen source for de novo glutamate synthesis (Pardo et al., 2011). Because fo the lack of neuronal aspartate, astrogial synthesis of glutamate and glutamine falls, and glutamine levels progressively decline in the aralar KO brain (Pardo et al., 2011). This points to a gradual impairment of glutamatergic transmission in these animals.

Taken together, the results indicate that the cortical neurons of the aralar KO mouse are metabolically impaired, fail to acquire processes, or show progressive signs of axonal neurodegeneration and are committed to develop impairment in glutamatergic transmission. In contrast, Purkinje neurons in the cerebellum show no evidence of neurofilament loss. Interestingly, the levels of their neurotransmitter, GABA, were also unchanged in the aralar KO brain (Pardo et al., 2011), possibly because GABA levels are maintained independently of the glutamate-glutamine cycle, as indicated in recent modelling studies (Occhipinti et al., 2010). The reasons why these cerebellar neurons seem to be spared in the aralar KO brain is still unknown. In the mouse, citrin is transcribed at very low levels in groups of neurons in the deep cerebellar nuclei (Contreras et al., 2010), although the levels of citrin protein are hardly detectable. Whether these citrin-expressing neurons or other possible NADH shuttle systems compensate for the loss of aralar in the cerebellum is still an open question. This is important, especially because, unlike the case in mouse, human AGC1 deficiency does not result in hypomyelination in the cerebellum (Wibom et al., 2009).

The aralar KO mice show a characteristic lack of myelination in all brain regions and a drastic decrease in brain myelin proteins and lipids (Jalil et al., 2005; Sakurai et al., 2010). The first human patient with a complete lack of AGC1 activity resulting from a homozygous loss-of-function mutation in Slc25a12 has a similar global lack of myelin (Wibom at al., 2009).

A first clue to the cause of hypomyelination is a drop in brain NAA levels starting at 10 days postnatally and reaching 25% of control values at 20 days. The loss in NAA was also found in neuronal cultures derived from these mice (Jalil et al., 2005). Aralar KO brains had also a yet more dramatic loss of aspartate at 10 days (to 20%), and, as brain aspartate levels keep increasing from 10 to 20 days postnatal in wild-type but not in aralar KO mice, the decrease in aspartate is more pronounced, to about 5%, at 20 days (Jalil et al., 2005). The lack of aspartate is due to a lack of synthesis of aspartate in the brain, because the brain has to produce its own aspartate when the blood–brain barrier completes its development in the postnatal brain (Liebner et al., 2008). Aspartate is predominantly a neuronal product (Urenjak et al., 1993; Jalil et al., 2005; Pardo et al., 2011), and it requires Aralar for synthesis in mitochondria and transport to the cytosol. NAA is also a predominantly neuronal product (Urenjak et al., 1993; Ariyannur et al., 2010a), which derives from aspartate and acetylCoA, thanks to aspartate N-acetyl-transferase, which is also largely, but not exclusively, neuronal (Urenjak et al., 1993; Bjartmar et al., 2001; Ariyannur et al., 2010a; Wiame et al., 2010). The exact location of aspartate N-acetyltransferase (NAT8L), whether mitochondrial or microsomal or both, is still questioned (Ariyannur et al., 2010a; Wiame et al., 2010). NAT8L requires aspartate as substrate either in mitochondria or in the cytosol, and both of these sources of aspartate are unavailable in aralar KO mice, insofar as the lack of mitochondrial uptake of glutamate hampers OAA transamination in mitochondria, and cytosolic aspartate requires aralar for its transfer to the cytosol.

There is evidence that NAA may serve as a precursor of myelin lipid synthesis by way of providing acetate to the oligodendrocyte. This relies on the transaxonal transport of NAA from neurons to oligodendrocytes, which have an NAA transporter, NaDC3; an Na^+-dependent, high-affinity dicarboxylate transporter (Huang et al., 2000); and, in the presence of aspartoacylase (ASPA), the NAA splitting enzyme, where its expression increases late during development (Dugas et al., 2006). Brain ASPA expression starts in the embryonic brain (Kumar et al., 2009) and peaks at 30 days, when myelin production is maximal (Mattan et al., 2010). Brain acetyl-CoA synthetase required to produce acetylCoA from free acetate also peaks at about postnatal day 18 and may also be involved in histone acetylation (Ariyannur et al., 2010b). Additional evidence indicating that NAA is an important source of myelin lipid synthesis derives from studies in murine models of Canavan disease (Matalon et al., 2000; Mattan et al., 2010), which causes the degeneration of the white matter, demyelination, and a spongy brain appearance. The disease is caused by mutations in ASPA, resulting in an accumulation of brain NAA and a reduction in brain acetate, the product of NAA breakdown (Blüml, 1999; Madhavaro et al., 2005). One possible pathogenic mechanism in Canavan disease is that excess NAA in brain is toxic (Kitada et al., 2000), perhaps to oligodendrocytes or oligodendrocyte precursor cells (OPCs). Because oligodendrocytes have NMDA receptors, and NAA can act on neuronal NMDA receptors, NAA may be toxic to oligodendrocytes by a mechanism similar to that involved in glutamate-induced neuronal death. This possibility has been ruled out, in that Kolodziejczyk et al. (2009) have found that NAA is not active on oligodendrocyte NMDA receptors. However, other pathogenic mechanisms of excess NAA cannot be excluded (Traka et al., 2008).

On the other hand, there is increasing evidence that ASPA deficiency causes impaired maturation of oligodendrocytes, with an increase in immature ones (Kumar et al., 2009; Mattan et al., 2010), because of a failure to take up sufficient acetate for myelin lipid synthesis (Madhavaro et al., 2005; Moffet et al., 2007). Some of these characteristics, such as the increase in immature oligodendrocytes, are shared with the CGT-KO mouse (Marcus and Popko, 2002) and the aralar KO mouse, suggesting that the effects on oligodendrocytes might occur through a partially common mechanism, involving a deficient substrate supply for myelin lipid synthesis.

It is, however, surprising that oligodendrocytes would use NAA rather than glucose for their own lipid synthesis, at least during development. One possibility is that NAA is used mainly in gray matter myelin, insofar as these are the regions most affected in the aralar KO mouse. The growing process in a myelinating oligodendrocyte is farthest apart from its own the cell body, but it lies in close contact with the axon around which it grows and wraps (Nave, 2010). As the oligodendrocyte process grows, local protein synthesis takes place there (Sherman and Brophy, 2005). It is possible that local lipid synthesis also occurs at the growing tip of the oligodendrocyte, using NAA from the axon that it wraps as precursor. NAA is produced at high levels in pyramidal neurons in cerebral cortex and other brain neurons also enriched in the enzyme responsible for NAA synthesis, NAT8L (Ariyannur et al., 2010a). It is possible that the growing tip of the oligodendrocyte is enriched in the NAA transporter NaDC3 and in aspartoacylase, which have been shown to be located not only in cell bodies but also in myelin (Chakraborty et al., 2001), to allow for local lipid synthesis away from the oligodendrocyte cell body. Interestingly, the mRNAs for the NAA transporter NaDC3 (Slc13a3), ASPA, acetyl-CoA synthetase (Acss2), and CGT (UGT8) are all substantially enriched (six- to 87-fold) in mouse brain myelinating oligodendrocytes compared with OPCs, whereas the expression of aralar and NAT8L is down-regulated (Cahoy et al., 2008).

On the other hand, it is unlikely that these restrictions in substrates for lipid synthesis can be recapitulated

in cultured oligodendrocytes, especially in a neuron-free culture. The serum-rich culture provides glucose, fatty acids and other nutrients, and it is likely that oligodendrocytes in mixed astroglial cultures use those during their maturation in culture. Therefore, the finding that oligodendrocytes from aralar KO mice develop normally in a neuron-free culture supports the idea that the defect in oligodendrocytes is due to a failure to receive NAA or other metabolites from aralar KO neurons in vivo rather than to an oligodendrocyte-specific defect. However, Sakurai et al. (2010) have reported that pure rat oligodendrocytes cultures in which aralar has been silenced do have a maturation defect. If this was also the case for mouse oligodendrocytes, the lack of aralar in oligodendrocytes, presumably in OPCs, which express both aralar (Cahoy et al., 2008) and NAT8L (Ariyannur et al., 2010a), might also be involved in the hypomyelination defect. Clearly, further studies are required to clarify this point.

ACKNOWLEDGMENTS

The CIBER de Enfermedades Raras is an initiative of the ISCIII. The authors thank Isabel Manso and Bárbara Sesé for technical support. I.L.-F. held a fellowship from the Comunidad de Madrid, Spain.

REFERENCES

Ariyannur PS, Moffett JR, Manickam P, Pattabiraman N, Arun P, Nitta A, Nabeshima T, Madhavarao CN, Namboodiri AMA. 2010a. Methamphetamine-induced neuronal protein NAT8L is the NAA biosynthetic enzyme: Implications for specialized acetyl coenzyme A metabolism in the CNS. Brain Res 1335:1–13.

Ariyannur PS, Moffett JR, Madhavarao CN, Arun Pishnu N, Jacobowitz DM, Hallows WC, Denu JM, Namboodiri AMA. 2010b. Nuclear-cytoplasmic localization of acetyl coenzyme a synthetase-1 in the rat brain. J Comp Neurol 518:2952–2977.

Bjartmar C, Battistuta J, Terada N, Dupree E, Trapp BD. 2002. N-acetylaspartate is an axon-specific marker of mature white matter in vivo: a biochemical and immunochemical study on the rat optic nerve. Ann Neurol 51:51–58.

Blüml S. 1999. In vivo quantitation of cerebral metabolite concentrations using natural abundance ^{13}C MRS at 1.5 T. J Magn Reson 136:219–225.

Bosio A, Binczek E, Stoffel W. 1996. Functional breakdown of the lipid bilayer of the myelin membrane in central and peripheral nervous system by disrupted galactocerebroside synthesis. Proc Natl Acad Sci U S A 93:13280–13285.

Butt AM, Ibrahim M, Berry M. 1997. The relationship between developing oligodendrocyte units and maturing axons during myelinogenesis in the anterior medullary velum of neonatal rats. J Neurocytol 26:327–338.

Cahoy JD, Emery B, Kaushal A, Foo LC, Zamanian JL, Christopherson KS, Xing Y, Lubischer JL, Krieg PA, Krupenko SA, Thompson WJ, Barres BA. 2008. A transcriptome database for astrocytes, neurons, and oligodendrocytes: a new resource for understanding brain development and function. J Neurosci 28:264–278.

Chakraborty G, Mekala P, Yahya D, Wu G, Ledeen RW. 2001. Intraneuronal N-acetylaspartate supplies acetyl groups for myelin lipid synthesis: evidence for myelin-associated aspartoacylase. J Neurochem 78:736–745.

Coetzee T, Fujita N, Dupree J, Shi R, Blight A, Suzuki K, Suzuki K, Popko B. 1996. Myelination in the absence of galactocerebroside and sulfatide: normal structure with abnormal function and regional instability. Cell 86:209–219.

Coetzee T, Dupree JL, Popko B. 1998. Demyelination and altered expression of myelin-associated glycoprotein isoforma in the central nervous system of galactolipid-deficient mice. J Neurosci Res 54:613–622.

Contreras L, Urbieta A, Kobayashi K, Saheki T, Satrústegui J. 2010. Low levels of citrin (SLC25A13) expression in adult mouse brain restricted to neuronal clusters. J Neurosci Res 88:1009–1016.

Dawson MRL, Levine JM, Reynolds R. 2000. NG2-expressing cells in the central nervous system: are they oligodendroglial progenitors? J Neurosci Res 61:471–479.

Dugas JC, Tai YC, Speed TP, Ngai J, Barres BA. 2006. Functional genomic analysis of oligodendrocyte differentiation. J Neurosci 26:10967–10983.

Dyer CA, Kendler A, Jean-Guillaume D, Awatramani R, Lee A, Mason LM, Kamholz J. 2000. GFAP-positive and myelin marker-positive glia in normal and pathologic environments. J Neurosci Res 60:412–426.

Huang W, Wang H, Kekuda R, Fei YJ, Friedrich A, Wang J, Conway SJ, Cameron RS, Leibach FH, Ganapathy V. 2000. Transport of N-acetylaspartate by the Na^+-dependent high-affinity dicarboxylate transporter NaDC3 and its relevance to the expression of the transporter in the brain. J Pharmacol Exp Ther 295:392–403.

Jalil MA, Begum L, Contreras L, Pardo B, Iijima M, Li MX, Ramos M, Marmol P, Horiuchi M, Shimotsu K, Nakagawa S, Okubo A, Sameshima M, Isashiki Y, Del Arco A, Kobayashi K, Satrústegui J, Saheki T. 2005. Reduced N-acetylaspartate levels in mice lacking aralar, a brain- and muscle-type mitochondrial aspartate-glutamate carrier. J Biol Chem 280:31333–31339.

Kitada K, Akimitsu T, Shigematsu Y, Kondo A, Maihara T, Yokoi N, Kuramoto T, Sasa M, Serikawa T. 2000. Accumulation of N-acetyl-L-aspartate in the brain of the tremor rat, a mutant exhibiting absence-like seizure and spongiform degeneration in the central nervous system. J Neurochem 74:2512–2519.

Kolodziejczyk K, Hamilton NB, Wade A, Karadottir R, Attwell D. 2009. The effect of N-acetyl-aspartyl-glutamate and N-acetyl-aspartate on white matter oligodendrocytes. Brain 132:1496–1508.

Kumar S, Biancotti JC, Matalon R, de Vellis J. 2009. Lack of aspartoacylase activity disrupts survival and differentiation of neural progenitors and oligodendrocytes in a mouse model of Canavan disease. J Neurosci Res 87:3415–3427.

LaNoue KF, Tischler ME. 1974. Electrogenic characteristics of the mitochondrial glutamate-aspartate antiporter. J Biol Chem 249:7522–7528.

Liebner S, Corada M, Bangsow T, Babbage J, Taddei A, Czupalla CJ, Reis M, Felici A, Wolburg H, Fruttiger M, Taketo MM, von Melchner H, Plate KH, Gerhardt H, Dejana E. 2008. Wnt/beta-catenin signaling controls development of the blood–brain barrier. J Cell Biol 183:409–417.

Madhavarao CN, Arun P, Moffett JR, Szucs S, Surendran S, Matalon R, Garbern J, Hristova D, Johnson A, Jiang W, Namboodiri MA. 2005. Defective N-acetylaspartate catabolism reduces brain acetate levels and myelin lipid synthesis in Canavan's disease. Proc Natl Acad Sci U S A 102:5221–5226.

Marcus J, Dupree JL, Popko B. 2000. Effects of galactolipid elimination on oligodendrocyte development and myelination. Glia 30:319–328.

Marcus J, Popko B. 2002. Galactolipids are molecular determinants of myelin development and axo-glial organization. Biochim Biophys Acta 1573:406–413.

Matalon R, Rady PL, Platt KA, Skinner HB, Quast MJ, Campbell GA, Matalon K, Ceci JD, Tyring SK, Nehls M, Surendran S, Wei J, Ezell EL, Szucs S. 2000. Knock-out mouse for Canavan disease: a model for gene transfer to the central nervous system. J Genet Med 2:165–175.

Mattan NS, Ghiani CA, Lloyd M, Matalon R, Bok D, Casaccia P, de Vellis J. 2010. Aspartoacylase deficiency affects early postnatal development of oligodendrocytes and myelination. Neurobiol Dis 40:432–443.

McCarthy KD, De Vellis J. 1980. Preparation of separate astroglial and oligodendroglial cell cultures fron rat cerebral tissue. J Cell Biol 85:890–902.

Mehta V, Namboodiri MA. 1995. N-acetylaspartate as an acetyl source in the nervous system. Brain Res Mol Brain Res 31:151–157.

Moffett JR, Ross B, Arun P, Madhavarao CN, Namboodiri AM. 2007. N-acetylaspartate in the CNS: from neurodiagnostics to neurobiology. Prog Neurobiol 81:89–131.

Molinari F, Raas-Rothschild A, Rio M, Fiermonte G, Encha-Razavi F, Palmieri L, Palmieri F, Ben-Neriah Z, Kadhom N, Vekemans M, Attie-Bitach T, Munnich A, Rustin P, Colleaux L. 2005. Impaired mitochondrial glutamate transport in autosomal recessive neonatal myoclonic epilepsy. Am J Hum Genet 76:334–339.

Molinari F, Kaminska A, Fiermonte G, Boddaert N, Raas-Rothschild A, Plouin P, Palmieri L, Brunelle F, Palmieri F, Dulac O, Munnich A, Colleaux L. 2009. Mutations in the mitochondrial glutamate carrier SLC25A22 in neonatal epileptic encephalopathy with suppression bursts. Clin Genet 76:188–194.

Nave K-A. 2010. Myelination and the trophic support of long axons. Nat Rev Neurosci 11:275–283.

Niwa M, Nitta A, Mizoguchi H, Ito Y, Noda Y, Nagai T, Nabeshima T. 2007. A novel molecule "shati" is involved in methamphetamine-induced hyperlocomotion, sensitization, and conditioned place preference. J Neurosci 27:7604–7615.

Occhipinti R, Somersalo E, Calvetti D. 2010. Energetics of inhibition: insights with a computational model of the human GABAergic neuron–astrocyte cellular complex. J Cerebr Blood Flow Metab 30:1834–1846.

Pardo B, Rodrigues TB, Contreras L, Garzón M, Llorente-Folch I, Kobayashi K, Saheki T, Cerdan S, Satrústegui J. 2011. Brain glutamine synthesis requires neuronal-born aspartate as amino donor for glial glutamate formation. J Cereb Blood Flow Metab 31:90–101.

Sakurai T, Ramoz N, Barreto M, Gazdoiu M, Takahashi N, Gertner M, Dorr N, Gama Sosa MA, De Gasperi R, Perez G, Schmeidler J, Mitropoulou V, Le HC, Lupu M, Hof PR, Elder GA, Buxbaum JD. 2010. Slc25a12 disruption alters myelination and neurofilaments: a model for a hypomyelination syndrome and childhood neurodevelopmental disorders. Biol Psychiatry 67:887–894.

Satrústegui J, Contreras L, Ramos M, Marmol P, del Arco A, Saheki T, Pardo B. 2007a. Role of aralar, the mitochondrial transporter of aspartate-glutamate, in brain N-acetylaspartate formation and Ca^{2+} signaling in neuronal mitochondria. J Neurosci Res 85:3359–3366.

Satrústegui J, Pardo B, del Arco A. 2007b. Mitochondrial transporters as novel targets for intracellular calcium signaling. Physiol Rev 87:29–67.

Sherman DL, Brophy PJ. 2005. Mechanisms of axon ensheathment and myelin growth. Nat Rev Neurosci 6:683–690.

Sommer I, Schachner M. 1981. Monoclonal antibodies (O1 to O4) to oligodendrocyte cell surfaces: An immunocytological study in the central nervous system. Dev Biol 83:311–327.

Traka MWollmann RL, Cerda SR, Dugas J, Barres BA, Popko B. 2008. Mur7 is a nonsense mutation in the aspartoacylae gene that cuases spongy degeneration of the CNS. J Neurosci 28:11537–11549.

Urenjak J, Williams SR, Gadian DG, Noble M. 1993. Proton nuclear magnetic resonance spectroscopy unambiguously identifies different neural cell types. J Neurosci 13:981–989.

Wiame E, Tyteca D, Pierrot N, Collard F, Amyere M, Noel G, Desmedt J, Nassogne MC, Vikkula M, Octave JN, Vincent MF, Courtoy PJ, Boltshauser E, van Schaftingen E. 2010. Molecular identification of aspartate N-acetyltransferase and its mutation in hypoacetylaspartia. Biochem J 425:127–136.

Wibom R, Lasorsa FM, Töhönen V, Barbaro M, Sterky FH, Kucinski T, Naess K, Jonsson M, Pierri CL, Palmieri F, Wedell A. 2009. AGC1 deficiency associated with global cerebral hypomyelination. N Engl J Med 361:489–495.

Woodruff RH, Tekki-Kessaris N, Stiles CD, Rowitch DH, Richardson WD. 2001. Oligodendrocyte development in the spinal cord and telencephalon: common themes and new perspectives. Int J Dev Neurosci 19:379–385.

Zöller I, Büssow H, Gieselmann V, Eckhardt M. 2005. Oligodendrocyte-specific ceramide galactosyltransferase (CGT) expression phenotypically rescues CGT-deficient mice and demonstrates that CGT activity does not limit brain galactosylceramide level. Glia 52:190–198.

Genotypic and phenotypic features of citrin deficiency: Five-year experience in a Chinese pediatric center

YUAN-ZONG SONG[1], MEI DENG[1], FENG-PING CHEN[2], FANG WEN[1], LI GUO[1], SHUI-LIANG CAO[6], JIAN GONG[3], HAO XU[3], GUANG-YU JIANG[4], LE ZHONG[7], KEIKO KOBAYASHI[8*], TAKEYORI SAHEKI[9] and ZI-NENG WANG[5]

Departments of [1]Pediatrics, [2]Laboratory Science, [3]Nuclear Medicine, [4]Pathology, [5]Gynecology and Obstetrics, The First Affiliated Hospital, and [6]Analytical and Testing Center, Jinan University, Guangzhou 510630; [7]Department of Pediatrics, Xiang-Ya Hospital, Central South University, Changsha 410008, P.R. China; [8]Department of Molecular Metabolism and Biochemical Genetics, Kagoshima University Graduate School of Medical and Dental Sciences, Kagoshima 890-8544; [9]Institute for Health Sciences, Tokushima Bunri University, Tokushima 770-8514, Japan

Received January 14, 2011; Accepted February 28, 2011

DOI: 10.3892/ijmm.2011.653

Abstract. Citrin is a liver-type aspartate/glutamate carrier (AGC) encoded by the gene SLC25A13. Two phenotypes for human citrin deficiency have been described, namely the adult-onset citrullinemia type II (CTLN2) and the neonatal intrahepatic cholestasis caused by citrin deficiency (NICCD). However, citrin deficiency currently remains a perplexing and poorly recognized disorder. In particular, description of post-NICCD clinical presentations before CTLN2 onset is rather limited. Analysis of SLC25A13 mutations, identification of dysmorphic erythrocytes, hepatobiliary scintigraphic imaging and investigation of post-NICCD clinical presentations were performed in a citrin-deficient cohort comprised of 51 cases of children diagnosed with citrin deficiency in a Chinese pediatric center. Twelve SLC25A13 mutations were detected in this cohort, including the novel V411M and G283X mutations. Among the 51 citrin-deficient subjects, 7 cases had echinocytosis, which was associated with more severe biochemical abnormalities. Delayed hepatic discharge and bile duct/bowel visualization were common scintigraphic findings. Moreover, 9 of the 34 post-NICCD cases demonstrated concurrent failure to thrive and dyslipidemia, constituting a clinical phenotype different from NICCD and CTLN2. The novel mutations, echinocytosis, hepatobiliary scintigraphic features and the novel clinical phenotype in this study expanded the genotypic and phenotypic spectrum of citrin deficiency, and challenge the traditionally-assumed 'apparently healthy' period after the NICCD state for this disease entity.

Correspondence to: Dr Yuan-Zong Song, Department of Pediatrics, The First Affiliated Hospital, Jinan University, No. 613 Huangpu Dadao Xi, Guangzhou 510630, Guangdong, P.R. China
E-mail: songyuanzong@tom.com

*Deceased

Abbreviations: NICCD, neonatal intrahepatic cholestasis caused by citrin deficiency; CTLN2, adult-onset citrullinemia type II; Tc-99m-EHIDA, technetium-99m-N,α-(2,6-diethylacetanilide)-iminodiacetic acid; SPECT, single-photon emission computed tomography; FTT, failure to thrive; FTTDCD, failure to thrive and dyslipidemia caused by citrin deficiency

Key words: citrin deficiency, neonatal intrahepatic cholestasis caused by citrin deficiency, SLC25A13, echinocytosis

Introduction

Citrin is a liver-type aspartate/glutamate carrier (AGC) encoded by the gene SLC25A13 which was cloned in 1999 by Kobayashi *et al* (1). It has been well-recognized that human citrin deficiency encompasses both adult-onset type II citrullinemia (CTLN2, OMIM #603471) and neonatal intrahepatic cholestasis caused by citrin deficiency (NICCD, OMIM #605814). An 'apparently healthy' period without symptoms between the state of NICCD and the onset of CTLN2 has been traditionally assumed for years (2). However, a potentially different course of citrin deficiency, including failure to thrive (FTT), hyperlipidemia, hepatoma and pancreatitis at the post-NICCD but pre-CTLN2 stage, has been proposed by Saheki *et al* (3), suggesting the existence of other post-NICCD phenotype(s) in addition to CTLN2. Although citrin deficiency was initially reported among individuals of East Asian ancestry, more and more citrin-deficient patients have been identified in other populations (4-10), suggesting it is a panethnic disease with a worldwide distribution. Further elucidation of the clinical and laboratory characteristics of this disease will facilitate its early diagnosis and appropriate management. Citrin deficiency currently remains a perplexing and poorly recognized disorder (11,12). In particular, a description of post-NICCD clinical presentations before CTLN2 onset is rather limited, although abnormal metabolic profiles at this stage have been reported by Nagasaka *et al* (13). We performed a comprehensive review in a citrin-deficient cohort obtained from a Chinese pediatric center, to explore

novel molecular, erythrocytic, scintigraphic and post-NICCD clinical features.

Subjects and methods

Subjects. This citrin-deficient cohort was composed of 51 pediatric cases diagnosed between July 2005 and September 2010 in the Department of Pediatrics, the First Affiliated Hospital, Jinan University, Guangdong, China. All diagnoses were confirmed by SLC25A13 analysis, and some genotypes had been reported in our previous publications (14-18). Galactose-free and/or medium-chain triglycerides (MCTs) enriched formulas were introduced as dietary therapeutics in most cases once their diagnoses were suspected or established. In some patients with obvious jaundice and cholestatic indices, oral ursodeoxycholate and intravenous reductive glutathione were given, and intravenous arginine was administered in several cases of hyperammonemia. All subjects were followed-up by counseling at the clinic and by e-mail or telephone counseling, and the clinical information was recorded in detail.

SLC25A13 mutation analysis. The four most frequent mutations, i.e. 851del4, 1638-1660dup, IVS6+5G>A and IVS16ins3kb, were screened by means of a routine procedure (15,16), and DNA sequencing of the 18 exons and their flanking sites in the SLC25A13 gene was performed as described in our previous investigations (17,18) in the subjects in which only one mutation was identified. Adhering to the principles of the Declaration of Helsinki, the parents of all subjects gave informed consents. This study has been approved by the Committee for Ethics of the Kagoshima University Faculty of Medicine in Japan, and by the Committee for Medical Ethics, the First Affiliated Hospital, Jinan University in China.

Light and electron microscopy. Blood smears were prepared with venous samples collected from the subjects. Erythrocyte morphology observation was performed after Giemsa staining by means of a previously described procedure (19). Scanning electron microscopy (SEM) was used to confirm the erythrocyte dysmorphy in some cases. SEM sample preparation, including erythrocyte fixing with glutaraldehyde, buffer washing, post-fixing with osmium tetroxide, dehydration with ethanol, depositing of a diluted sample drop, air drying and coating with gold, was carried out as previously described (20). A Nikon Eclipse 80i (Japan) microscope and a Philips ESEM XL-30 SEM instrument (The Netherlands) were used for the analysis. The echinocyte stages were classified according to Brecher *et al* (21): stage 1 is characterized by irregularity of cellular edges; stage 2 by spicules in a still flat cell; and stage 3 by spicules uniformly distributed over the surface of a round cell.

Hepatobiliary scintigraphic imaging. Scintigraphy of the hepatobiliary system with technetium-99m-N,α-(2,6- diethyl-acetanilide)-iminodiacetic acid (Tc-99m-EHIDA) as the tracer has been well recognized as a reliable tool for clinical investigation of the origin of jaundice. To distinguish between the icterus of a hepatocellular and an obstructive origin, Tc-99m-EHIDA was injected intravenously at the dosage of 1 mCi, and serial abdominal views were obtained by means of a scintillation camera, during at least the first hour and up to 24 h when necessary. A single-photon emission computed tomography (SPECT) instrument (Elscint Helix, GE Healthcare) was used in this study to perform hepatobiliary imaging.

Clinical presentations after the NICCD state. We investigated the clinical features of the citrin-deficient subjects after the NICCD state, focusing on their anthropometric and biochemical information collected in the past five years. In this study, measurements of weight- and/or length-for-chronological age <5th percentile were defined as FTT according to Olsen *et al* (22), and the age and gender-matched 5th percentile values of the anthropometric indices were based on the WHO child growth standards (http://www.who.int/childgrowth/standards/en/). Furthermore, patients with serum levels of total triglycerides (TG) ≥1.70 mmol/l, and/or total cholesterol (T-Chol) ≥5.18 mmol/l, and/or high density lipoprotein (HDL)-cholesterol ≤1.04 mmol/l and/or low density lipoprotein (LDL)-cholesterol ≥3.37 mmol/l, were defined as dyslipidemic (23).

Statistics. Independent-sample t-tests were used to compare the differences of serum biochemical indices between different groups of patients with and without echinocytosis, and those with and without failure to thrive and dyslipidemia caused by citrin deficiency (FTTDCD). The indices following a Gaussian distribution are presented as the mean ± SD, and those skewed are denoted as the median (minimum, maximum). Skewed raw data were logarithmically transformed before statistical assessment as indicated in the corresponding tables. The difference in the SLC25A13 mutation spectrum was examined by using the latitude of 30°N as the border line dividing the patient origin between the south or north China. The mutation spectrum difference was evaluated by means of a 2x2 table χ^2-test with correction for continuity. A P-value <0.05 was taken to denote statistical significance.

Results

Patient information. The subjects came from 13 provinces, municipalities and autonomous regions of mainland China, including Guangdong, Guangxi, Hunan, Hubei, Jiangxi, Shanghai, Jiangsu, Zhejiang, Fujian, Shandong, Shanxi, Henan and Hebei, with most of them from south China (south of 30°N) such as the Guangdong and Hunan provinces. As listed in Table I, the citrin-deficient cohort in this study was composed of 51 subjects including 17 females and 34 males, with NICCD as the main clinical presentation in most cases. Three subjects demonstrated poor outcomes and another 2 lost contact, but all the remaining 46 cases recovered or improved clinically. However, FTT and dyslipidemia were observed as rather common manifestations after the NICCD state, as described in detail below.

SLC25A13 mutations. A total of 12 mutations including the 7 previously reported mutations (14-18), 851del4, IVS6+5G>A, 1638-1660dup, IVS16ins3kb, G333D, A541D and R319X, and 5 additional ones, IVS11+1G>A, R360X, R467X, V411M and G283X, were found in this Chinese cohort, as shown

Table I. General information and SLC25A13 mutations in the citrin-deficient cohort.

Case	Patient	Gender	Mutations[a]	Major presentations	Clinical outcomes
01	P1071	Male	851del4/1638-1660dup	NICCD	Normal
02	P1194	Female	851del4/A541D	NICCD	Normal
03	P1194S	Female	851del4/A541D	NICCD	Normal
04	P1443	Male	IVS6+5G>A/R319X	NICCD	Died of ICI
05	P1478	Female	851del4/851del4	NICCD	Normal
06	P1482	Male	851del4/851del4	NICCD	Lost contact
07	P1495	Female	851del4/G333D	NICCD	Normal
08	P1513	Female	851del4/IVS16ins3kb	NICCD	Normal
09	P1628	Male	851del4/IVS6+5G>A	NICCD	FTT, dyslipidemia
10	P1638	Male	851del4/1638-1660dup	NICCD	FTT
11	P1643	Female	851del4/**?**	NICCD	FTT, dyslipidemia
12	P1644	Female	851del4/IVS6+5G>A	NICCD	Lost contact
13	P1648	Male	851del4/851del4	NICCD	FTT, dyslipidemia
14	P1751	Male	IVS6+5G>A/**?**	NICCD	Died of DIC
15	P1752	Female	851del4/851del4	NICCD	Normal
16	P1863	Male	851del4/IVS6+5G>A	NICCD	Normal
17	P1883	Male	851del4/IVS16ins3kb	NICCD	FTT
18	P1933	Male	851del4/IVS16ins3kb	NICCD	FTT, dyslipidemia
19	P1945	Female	IVS6+5G>A/**?**	NICCD	Normal
20	P1946	Male	851del4/851del4	NICCD	Normal
21	P1947	Male	851del4/851del4	NICCD	Normal
22	P1518	Male	851del4/851del4	FTT, dyslipidemia	Normal
23	C0002	Male	IVS11+1G>A/R360X	NICCD	Normal
24	C0004	Female	851del4/851del4	NICCD	Normal
25	C0005	Male	851del4/IVS6+5G>A	NICCD	FTT, dyslipidemia
26	C0006	Male	851del4/R467X	NICCD	Normal
27	C0009	Male	851del4/851del4	NICCD	Normal
28	C0010	Male	1638-1660dup/IVS6+5G>A	NICCD	Normal
29	C0012	Female	851del4/***V411M***	NICCD	Improved cholestasis, FTT
30	C0013	Male	851del4/851del4	Liver cirrhosis, FTT, GDD	Dyslipidemia, died of hepatic encephalopathy
31	C0016	Male	851del4/851del4	NICCD	FTT, Transient GDD
32	C0018	Female	851del4/***G283X***	NICCD	Normal
33	C0019	Male	851del4/R467X	NICCD	Motor retardation, dyslipidemia
34	C0020	Male	851del4/851del4	NICCD	Normal
35	C0021	Male	851del4/IVS16ins3kb	NICCD	Normal
36	C0025	Male	851del4/851del4	NICCD	Improved, FTT
37	C0027	Male	851del4/851del4	NICCD	Improved cholestasis
38	C0028	Male	851del4/851del4	NICCD	Improved cholestasis
39	C0029	Male	851del4/851del4	NICCD	Improved cholestasis
40	C0030	Female	851del4/851del4	NICCD	FTT, dyslipidemia
41	C0031	Male	1638-1660dup/IVS16ins3kb	NICCD	Improved cholestasis
42	C0032	Male	851del4/1638-1660dup	NICCD	Improved cholestasis
43	C0033	Female	851del4/851del4	NICCD	Improved cholestasis
44	C0035	Male	851del4/IVS16ins3kb	NICCD	Improved cholestasis
45	C0036	Male	851del4/851del4	NICCD	Improved cholestasis
46	C0037	Male	851del4/851del4	NICCD	FTT, dyslipidemia
47	C0041	Male	851del4/1638-1660dup	NICCD	Improved cholestasis
48	C0042	Male	851del4/1638-1660dup	NICCD	Improved cholestasis
49	C0043	Female	851del4/**?**	NICCD	Improved cholestasis
50	C0044	Female	851del4/851del4	NICCD	Improved cholestasis
51	C0046	Female	1638-1660dup/IVS6+5G>A	NICCD	Improved cholestasis

[a]The mutations in cases 1-22, 30 and 31 have been previously reported (14-18). Bold italic letters indicate the two novel mutations; the bold question marks indicate the unknown mutations. NICCD, neonatal intrahepatic cholestasis caused by citrin deficiency; FTT, failure to thrive; ICI, intracranial infection; DIC, disseminated intravascular coagulation; GDD, gross developmental delay.

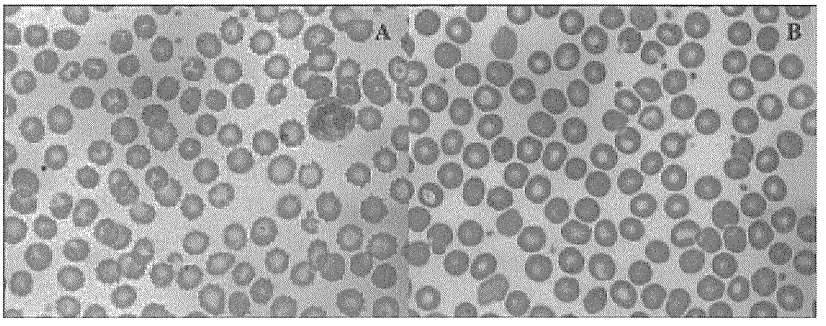

Figure 1. Light micrographs of echinocytosis in a male infant (C0016) with citrin deficiency. (A) Giemsa staining of blood smears demonstrating numerous echinocytes (x1000) at his age of 5.5 months. (B) Normalized erythrocyte morphology (x1000) when the biochemical and clinical abnormalities improved 2 months later.

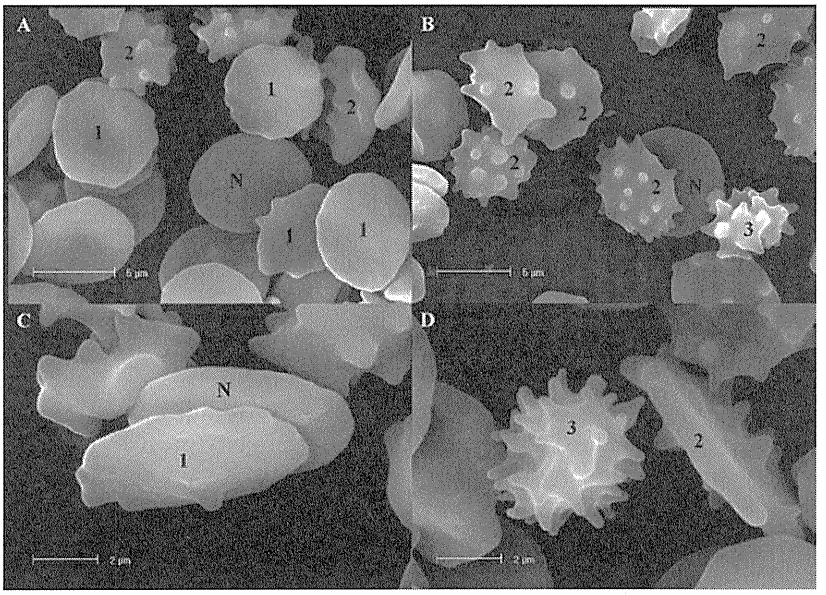

Figure 2. Scanning electron micrographs of echinocytosis in a citrin-deficient infant (C0027). The patient is a 4.5 month-old male. Numbers 1, 2 and 3 indicate echinocytes at stages 1, 2 and 3, respectively, with N representing normal erythrocytes. Magnification: x5000 in A and B, and x10000 in C and D.

in Table I. As far as we know, V411M and G283X are novel mutations never reported before. With regard to the frequency of the mutations, the 4 most frequent mutations 851del4, IVS6+5G>A, IVS16ins3kb and 1638-1660dup took account for 87%, while the remaining mutations occupied only 13% of the total 100 mutant SLC25A13 alleles (P1194 and P1194S from the same family). The distribution of SLC25A13 mutations in north and south China was compared using the latitude 30°N as the dividing line, and the 4 most frequent mutations occupied a proportion of 92.8% vs. 58.5% of the total amount of SLC25A13 mutations identified in citrin-deficient patients from south and north China, respectively. The distribution difference was significant statistically, with χ^2-value of 11.53 and $P<0.005$.

Echinocytosis. Microscopic observation of the morphology of erythrocytes was conducted in 22 citrin-deficient children, and echinocytosis was found in 7 cases. Echinocytosis was transient and resolved along with their biochemical and clinical improvement in 6 cases but one toddler (C0013) with persistent echinocytosis had a lethal outcome at 1 year and 10 months of age due to cirrhosis. Representative micrographic changes of echinocytosis in a citrin-deficient subject (C0016) are illustrated in Fig. 1, and in Fig. 2, echinocytes at different stages in another citrin-deficient infant (C0027) are illustrated as the means of SEM. We compared the serum biochemical indices between the citrin-deficient subjects with and without echinocytosis. As shown in Table II, patients with echinocytosis demonstrated more severe biochemical abnormalities, including higher serum levels of AST, TBil, DBil, AFP and ApoB100 and lower levels of HDL-Chol and ApoA1.

Tc-99m-EHIDA scintigraphic findings. We describe the features of hepatobiliary scintigraphy performed in 8 NICCD subjects (P1513, P1945, C0002, C0025, C0032, C0037, C0042 and C0046). Patient C0025 (Fig. 3) demonstrated impaired hepatic uptake of Tc-99m-EHIDA and consequently a failure of bile duct and bowl visualization before treatment. Delayed hepatic discharge and delayed/weak bile duct and bowel visualization still existed regardless of the significant improvement in the hepatic uptake at his discharge. Similar findings were observed in patient C0046. The remaining 6 citrin-deficient patients did not present with impaired hepatic uptake, however, delayed hepatic discharge and delayed/